TOTAL IONIZING DOSE TEST REPORT

No. 10T-RTAX1000S-CQ352-D4M9J1
Sept 27, 2010
J.J. Wang
(650) 318-4576
jih-jong.wang@actel.com

I. SUMMARY TABLE

Table 1 summarizes the TID tolerance for each tested parameters. The overall tolerance is limited by the standby power-supply current (I_{CC}). Because of logistical limitations, the room temperature annealing allowed by TM1019 to anneal down I_{CC} is performed for approximately 10 days. Every DUT passes all the listed specs in Table 1 for 300 krad(SiO_2) irradiation.

Table 1 Tolerances for each tested parameter

Parameter	Tolerance
1. Functionality	Passed 300 krad(SiO_2)
2. Standby Power Supply Current (I_{CCA}/I_{CCI})	Passed 200 krad(SiO_2)
3. Input Switching Threshold (V_{IHL}/V_{ILH})	Passed 300 krad(SiO_2)
4. Output Threshold (V_{OL}/V_{OH})	Passed 300 krad(SiO_2)
5. Propagation Delay	Passed 300 krad(SiO_2) for ±10% degradation criterion
6. Transition Time	Passed 300 krad(SiO_2)

II. TOTAL IONIZING DOSE (TID) TESTING

This section describes device under test (DUT), irradiation facility and parameters, test method, test design, and electrical parameter measurements. This TID testing, in various slightly modified forms, have been used to accumulate an extensive TID database for many generations of antifuse-based FPGAs; the link to access this TID database is attached in below:

http://www.actel.com/products/milaero/hireldata.aspx#tid

A. Device-Under-Test (DUT) and Irradiation Parameters

The part name of the DUTs is RTAX1000S; the package is CQ352. UMC used 0.15 µm technologies to manufacture it. This particular lot is numbered D4M9J1.

The Gamma Irradiator in radiation facility of Defense Microelectronics Activity is used to irradiate DUTs with Gamma rays: number 2517, 2518 and 2519 to 200 krad(SiO_2); number 2457, 2460 and 2516 to 300 krad(SiO_2). The dose rate is constant at 5 krad(SiO_2)/min (TM1019.8, condition A), and the ambiernt temperature is at 25°C.

B. Test Method

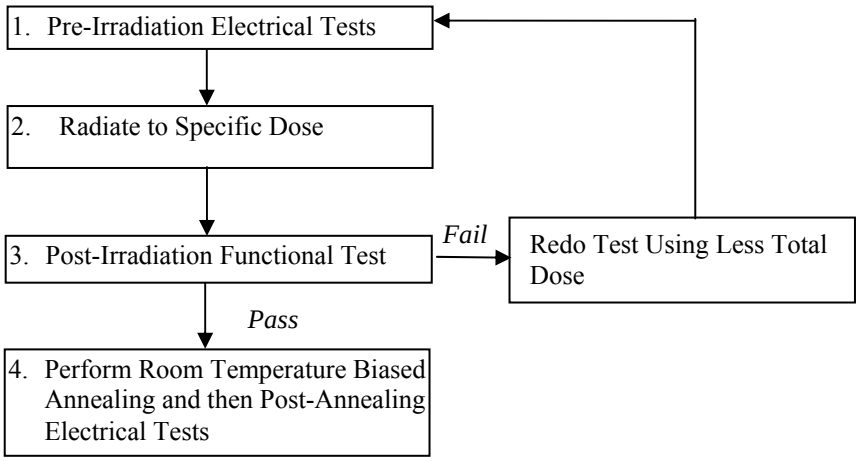

Figure 1 Parametric test flow chart

The test method is based on the military standard TM1019.8. Figure 1 shows the test flow. During irradiation, the DUT is statically biased with V_{CCI}/V_{CCA} = 3.3V/1.5V and all the inputs grounded. The accelerated annealing test in TM1019.8, section 3.12 has been done on sample lots of RTAXS, and the results show that post-irradiation annealing recovers the electrical characteristics rather than adversely affects the electrical performance. This is consistent with the general belief that the dominant TID effects in deep submicron CMOS devices are due to FOX-hole-trapping induced leakage currents and these leakages decrease with annealing temperatures. For a lot-to-lot testing such as the one in this report, the accelerated annealing test is omitted because it has been confirmed by the above information that the annealing effect is not adverse.

TM1019.8, Section 3.11 "extended room temperature anneal test" has been applied for approximately 10-days of annealing. The data measured after this annealing is named "Post Annealing" in section III Test Results.

C. DUT Logic Design

The DUT design is a high-utilization and generic design. It is similar to the design for RTAX2000S_CG624. Figure 2 shows a block diagram of the design for RTAX2000S_CG624; the Verilog file (rtax2000_CG624_Top.v) is in the aforementioned link or can be provided upon request. The functional test is performed on every sub-design with inputs and outputs; most inputs, including global clocks, are tested for leakage current; selected inputs are tested for threshold voltage, the standby I_{CC} test includes measuring static IO current (I_{CCI}) and static logic array current (I_{CCA}). Except propagation delay and the transition characteristic, which are measured on bench from the output pin O_BS, all parameter measurements are performed on a tester. Also note that, due to logistics limitation, the post-irradiation but pre-room-temperature-annealing functional test is performed on bench by measuring the expected outputs of shift registers and the long buffer string (sub-design 5 and 6 described in the following).

Sub-design 1 Embedded SRAM

This is to test the function of the embedded RAM. It uses all RAM blocks available in the DUT. This design enables an automatic testing sequence that every bit is written and then read. Any error will be reported as a signal in the output.

Sub-design 2 Unidirectional LVTTL Inputs and Outputs

This is for testing radiation effects on unidirectional input and output threshold, leakage, and buffer fan-out. LVTTL is used because it is the worst case among all the single-ended standards.

Sub-design 3 3.3V-LVPECL Input

This is for testing the radiation effects on the LVPECL differential inputs. 3.3V-LVPECL is considered the worst possible differential input standard. There are 7 channels.

Sub-design 4 Shift Registers

This is to test the radiation effects on the function of flip-flops, which are configured R-Cells.

Sub-design 5 Long Buffer String

This is to measure the radiation effects on the propagation delay. A clock signal feeding a toggle flip-flop generates a checkerboard signal; this signal is then fed into a buffer string with approximately 2,500 stages. The time delay between the input clock edge and the output switching at the end of the buffer string due to this clock edge is defined as propagation delay, which can be high to low (T_{pdhl}) or low to high (T_{pdlh}); the percentage change of the average of T_{pdhl} and T_{pdlh} is used to determine the total-dose tolerance. The total dose to cause 10% of propagation degradation is considered as the critical tolerance.

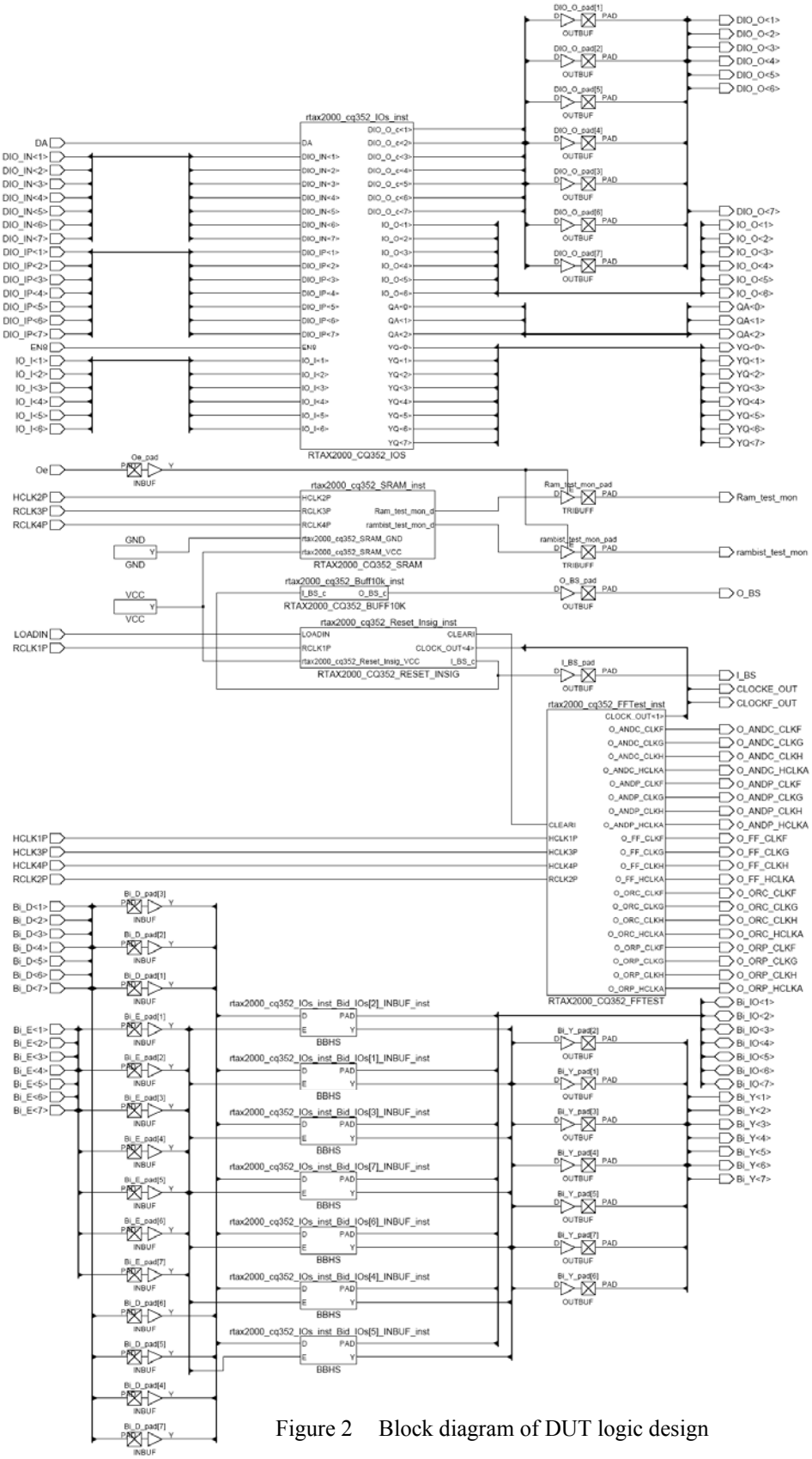

Figure 2 Block diagram of DUT logic design

III. TEST RESULTS

The test results mainly compare the electrical parameter measured pre-irradiation with the same parameter measured post-irradiation-and-annealing, or post-annealing. As mentioned previously, right after the irradiation and before annealing only the functionality of shift registers and long buffer string were tested on bench.

A. Functional Test

Every DUT passed the pre-irradiation and post-annealing functional tests on the tester. Every DUT also passed post-irradiation and pre-annealing functional tests of the shift registers and buffer string by using a bench setup.

B. Standby Power Supply Current (I_{CCA} and I_{CCI})

The logic-array power supply, V_{CCA}, is 1.5V, and the IO power supply, V_{CCI}, is 3.3V. Their standby currents, I_{CCA} and I_{CCI}, are monitored in-flux; Figure 3-8 show the plots of I_{CCA} and I_{CCI} versus total dose for the DUTs.

Referring to TM1019.8 subsection 3.11.2.c, the post-irradiation-parametric limit (PIPL) for the post-annealing I_{CC} should be defined as the addition of highest I_{CCI}, I_{CCDA} and $I_{CCDIFFA}$ values in Table 2-4 of the RTAXS spec sheet in the document posted on the Actel website; the link is attached in below:

http://www.actel.com/documents/RTAXS_DS.pdf

Therefor, the PIPL for I_{CCA} is 500 mA, and the PIPL of I_{CCI} is $35+10+3.13\times7 = 66.91$(mA). Note that there are 7 pairs of differential LVPECL inputs in each DUT.

Table 2 summarizes the pre-irradiation, post-irradiation—right after irradiation and before annealing, and post-annealing I_{CCA} and I_{CCI} data: the post-annealing I_{CCA} or I_{CCI} of every DUT, either irradiated to 200 krad(SiO_2) or 300 krad(SiO_2) is below the PIPL.

Table 2 Pre-irradiation, Post Irradiation and Post-Annealing I_{CCA} and I_{CCI}

DUT	Total Dose krad (SiO_2)	I_{CCA} (mA)			I_{CCI} (mA)		
		Pre-irrad	Post-irrad	Post-ann	Pre-irrad	Post-irrad	Post-ann
2457	300	6	69	17	28	142.5	69
2460	300	7	95	17	29	131.7	55
2516	300	3.5	132.6	20	27	135.2	63
2517	200	5	10.8	6	27	57.8	34
2518	200	7.3	10.2	10	27.7	58	36
2519	200	9	12.1	11	27.5	61.1	38

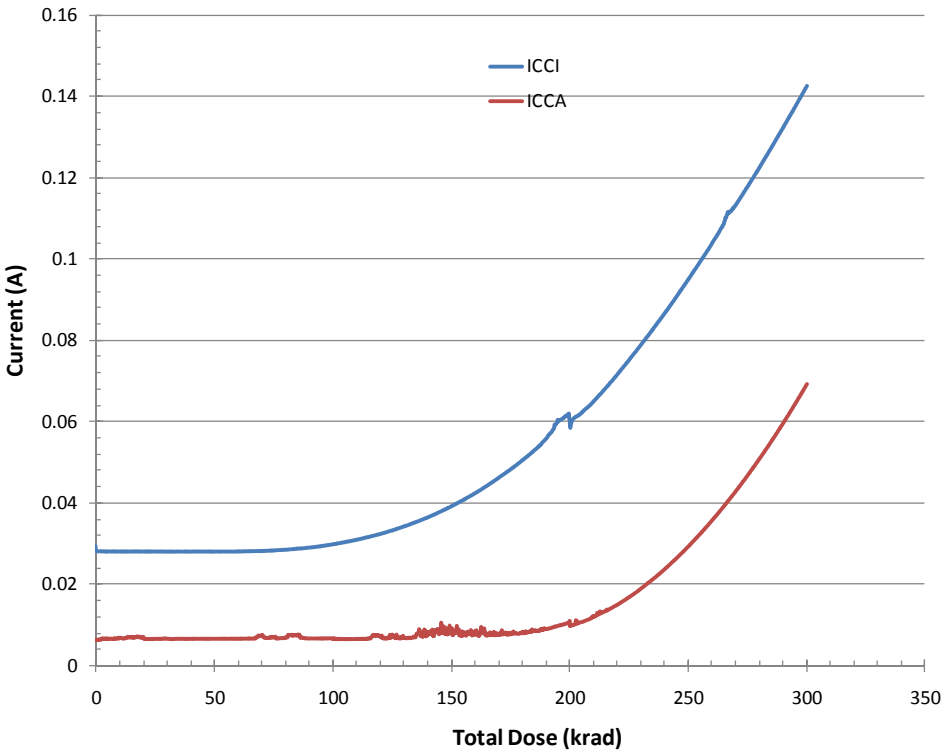

Figure 3 DUT 2457 in-flux I_{CCA} and I_{CCI}. If there is any curve-kink occurring at 100 krad or 200 krad, it is due to stopping irradiation for propagation-delay measurement.

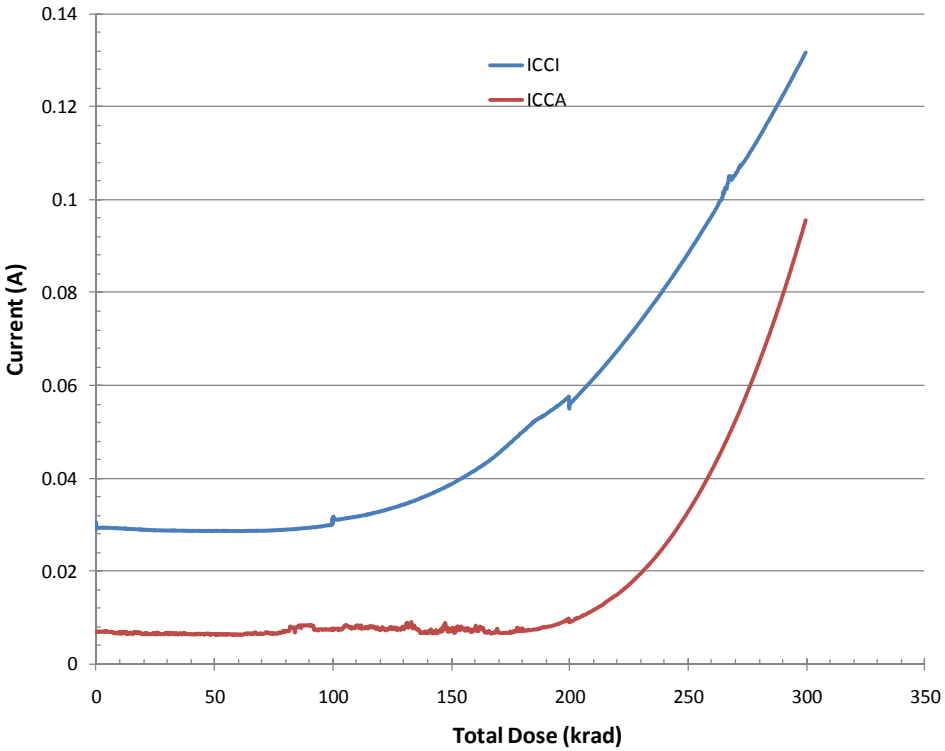

Figure 4 DUT 2460 in-flux I_{CCA} and I_{CCI}. If there is any curve-kink occurring at 100 krad or 200 krad, it is due to stopping irradiation for propagation-delay measurement.

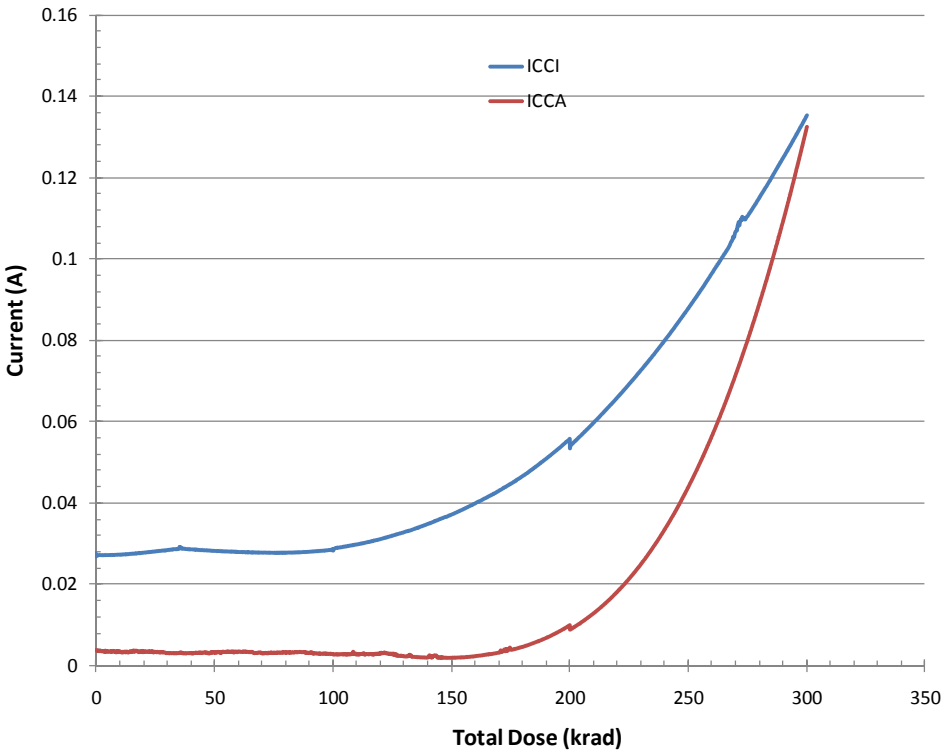

Figure 5 DUT 2516 in-flux I_{CCA} and I_{CCI}. If there is any curve-kink occurring at 100 krad or 200 krad, it is due to stopping irradiation for propagation-delay measurement.

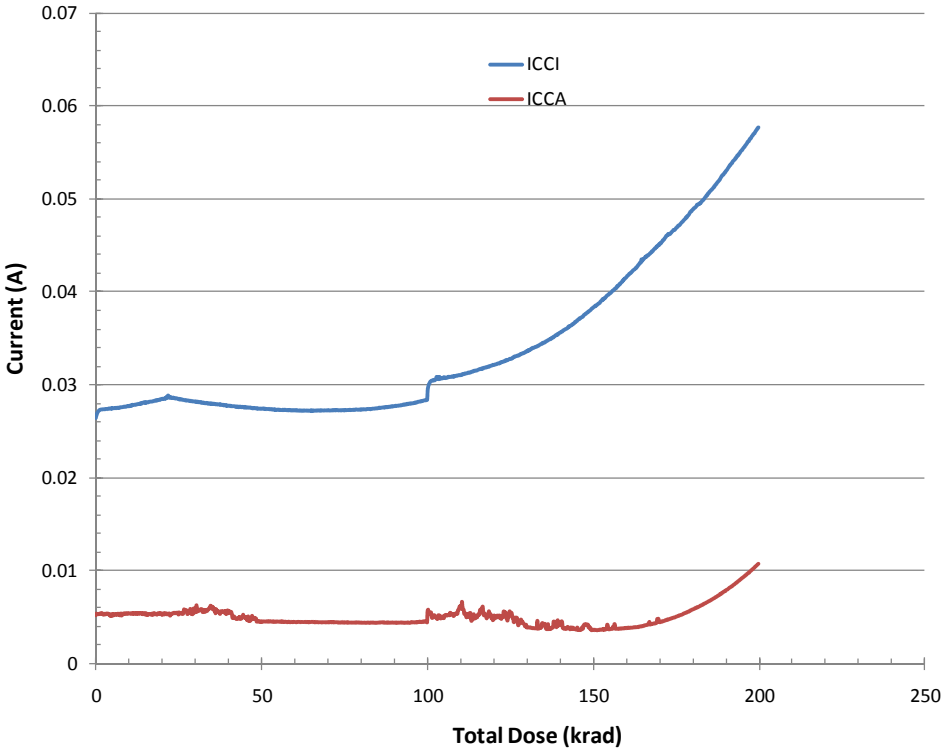

Figure 6 DUT 2517 in-flux I_{CCA} and I_{CCI}. If there is any curve-kink occurring at 100 krad, it is due to stopping irradiation for propagation-delay measurement.

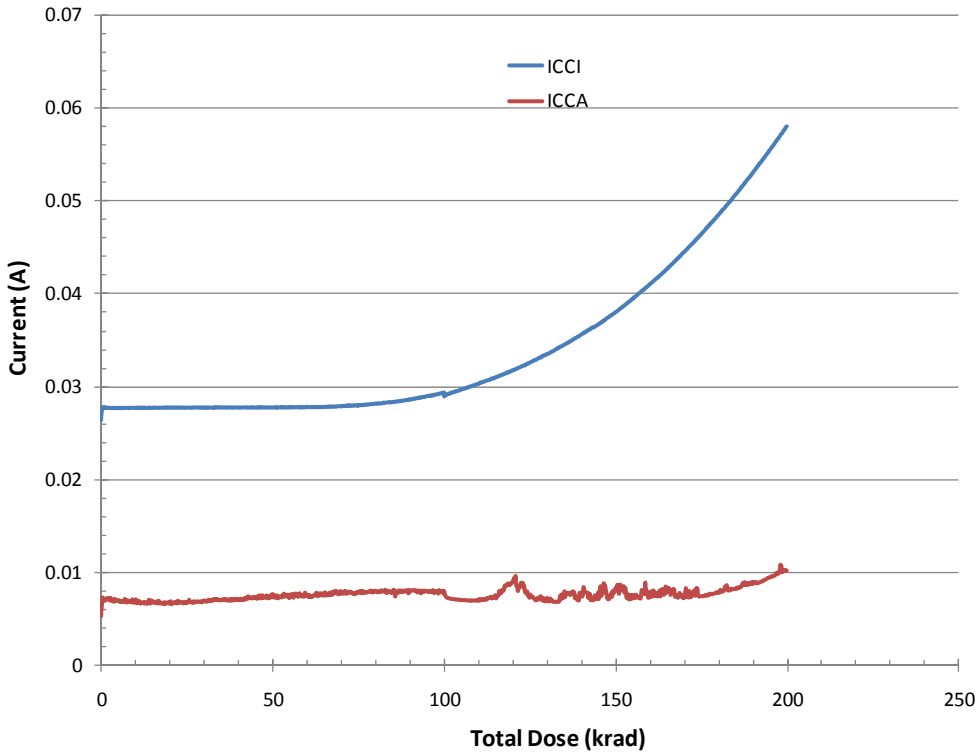

Figure 7 DUT 2518 in-flux I_{CCA} and I_{CCI}. If there is any curve-kink occurring at 100 krad, it is due to stopping irradiation for propagation-delay measurement.

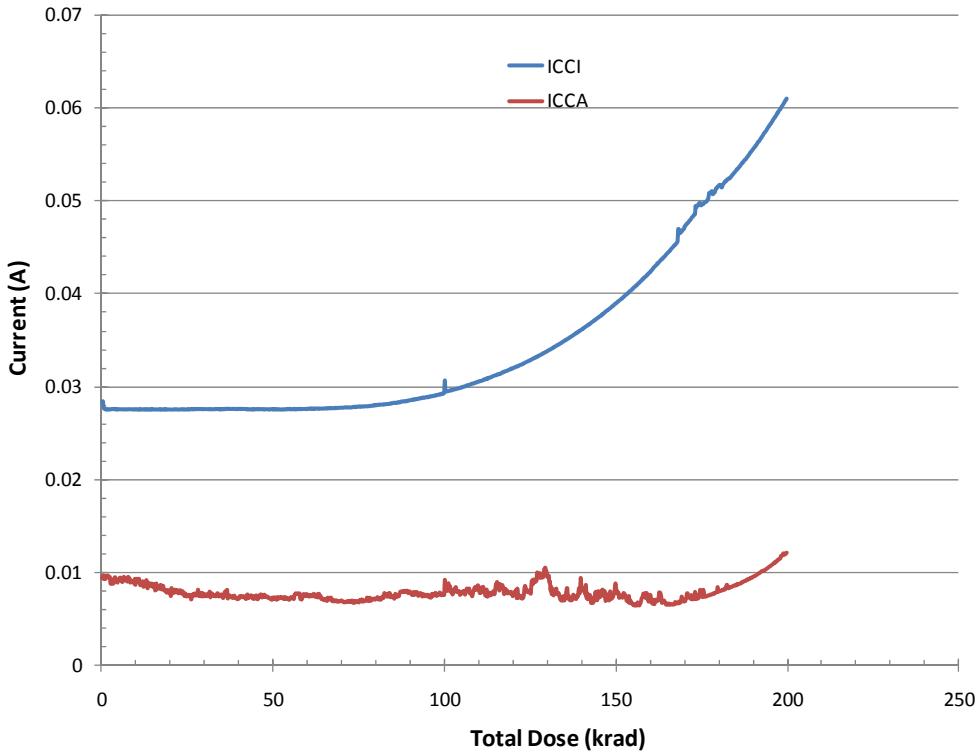

Figure 8 DUT 2519 in-flux I_{CCA} and I_{CCI}. If there is any curve-kink occurring at 100 krad, it is due to stopping irradiation for propagation-delay measurement.

C. *Single-Ended 3.3V-LVTTL V_{IL}/V_{IH} and I_{IL}/I_{IH}*

The input switching thresholds, or trip point, is defined as the applied input voltage at which the output of the design—often just input and output buffers—starts to switch: V_{IL} is the input trip point when the input is going high to low; V_{IH} is the input trip point when the input is going low to high. The power supplies for V_{IL}/V_{IH} measurement are set as:

$$V_{CCA}/V_{CCI}/V_{PP}/V_{SV}/V_{KS} = 1.4/3.0/1.5/1.5/0.0 \text{ V}$$

The power supplies for I_{IL}/I_{IH} measurement are set as:

$$V_{CCA}/V_{CCI}/V_{PP}/V_{SV}/V_{KS} = 1.5/3.3/1.5/1.5/0.0 \text{ V}$$

Tables 3a and 3b list the pre-irradiation and post-annealing single-ended V_{IL}. In each case, the difference between the pre-irradiation and post-annealing data is negligibly small. Tables 4a and 4b show the pre-irradiation and post-annealing single-ended V_{IH}; again the difference between the pre-irradiation and post-annealing data is negligibly small.

I_{IL} is the current sink into an input being forced to low, and I_{IH} is the current source from an input being forced to high. The PIPL for both of them is 5µA.

Tables 5a and 5b show the pre-irradiation and the post-annealing I_{IL} data. Tables 6a and 6b show the pre-irradiation and post-annealing I_{IH} data. The post-annealing data of both I_{IL} and I_{IH} for every tested input in every DUT is below the 5µA PIPL.

Table 3a Single-ended V_{IL} (V)

	2457		2460		2516		2517	
	Pre-Irra	Pos-Ann	Pre-Irra	Pos-Ann	Pre-Irra	Pos-Ann	Pre-Irra	Pos-Ann
DA	1.42	1.395	1.41	1.385	1.395	1.375	1.41	1.39
EN8	1.4	1.375	1.39	1.365	1.385	1.36	1.39	1.375
IO_I_6	1.415	1.39	1.405	1.385	1.395	1.375	1.405	1.385
IO_I_5	1.405	1.39	1.395	1.38	1.39	1.375	1.4	1.385
IO_I_4	1.42	1.395	1.41	1.385	1.39	1.375	1.4	1.39
IO_I_3	1.38	1.355	1.37	1.345	1.36	1.335	1.37	1.355
IO_I_2	1.41	1.39	1.405	1.385	1.395	1.37	1.405	1.38
IO_I_1	1.41	1.39	1.4	1.38	1.395	1.37	1.4	1.385
RCLK1P	1.44	1.44	1.43	1.43	1.43	1.43	1.425	1.42
RCLK2P	1.445	1.44	1.43	1.43	1.43	1.43	1.425	1.42
LOADIN	1.42	1.4	1.405	1.39	1.4	1.38	1.41	1.4

Table 3b Single-ended V_{IL} (V)

	2518		2519	
	Pre-Irra	Pos-Ann	Pre-Irra	Pos-Ann
DA	1.405	1.39	1.4	1.385
EN8	1.4	1.375	1.385	1.36
IO_I_6	1.405	1.395	1.4	1.38
IO_I_5	1.395	1.385	1.39	1.38
IO_I_4	1.4	1.39	1.395	1.385
IO_I_3	1.38	1.355	1.365	1.34
IO_I_2	1.4	1.39	1.395	1.375
IO_I_1	1.4	1.39	1.395	1.38
RCLK1P	1.435	1.435	1.43	1.43
RCLK2P	1.44	1.435	1.43	1.43
LOADIN	1.415	1.4	1.4	1.385

Table 4a Single-ended V_{IH} (V)

	2457		2460		2516		2517	
	Pre-Irra	Pos-Ann	Pre-Irra	Pos-Ann	Pre-Irra	Pos-Ann	Pre-Irra	Pos-Ann
DA	1.415	1.39	1.405	1.38	1.395	1.37	1.4	1.38
EN8	1.425	1.395	1.41	1.385	1.4	1.365	1.395	1.385
IO_I_6	1.42	1.395	1.41	1.385	1.4	1.375	1.41	1.39
IO_I_5	1.43	1.405	1.42	1.39	1.405	1.38	1.415	1.395
IO_I_4	1.42	1.395	1.415	1.385	1.4	1.375	1.41	1.39
IO_I_3	1.45	1.42	1.365	1.41	1.425	1.395	1.435	1.41
IO_I_2	1.43	1.4	1.425	1.395	1.415	1.385	1.425	1.4
IO_I_1	1.43	1.4	1.41	1.39	1.41	1.38	1.415	1.395
RCLK1P	1.645	1.62	1.625	1.605	1.625	1.61	1.62	1.61
RCLK2P	1.515	1.49	1.51	1.48	1.505	1.48	1.49	1.475
LOADIN	1.435	1.41	1.425	1.405	1.415	1.39	1.425	1.41

Table 4b Single-ended V_{IH} (V)

	2518		2519	
	Pre-Irra	Pos-Ann	Pre-Irra	Pos-Ann
DA	1.4	1.385	1.43	1.38
EN8	1.41	1.395	1.43	1.38
IO_I_6	1.405	1.39	1.4	1.385
IO_I_5	1.41	1.4	1.385	1.39
IO_I_4	1.405	1.39	1.405	1.385
IO_I_3	1.435	1.42	1.43	1.41
IO_I_2	1.42	1.4	1.415	1.385
IO_I_1	1.41	1.4	1.41	1.39
RCLK1P	1.62	1.615	1.625	1.615
RCLK2P	1.495	1.49	1.495	1.485
LOADIN	1.42	1.41	1.415	1.395

Table 5a Single-ended I_{IL} (nA)

	2457		2460		2516		2517	
	Pre-Irra	Pos-Ann	Pre-Irra	Pos-Ann	Pre-Irra	Pos-Ann	Pre-Irra	Pos-Ann
DA	-11.0441	-5.8219	-6.0156	-7.4974	-3.0824	-6.8691	-7.6918	-5.403
RCLK1P	-8.613	0.8648	-6.3088	-0.1824	-7.7751	0.027	-5.052	-3.1146
IO_I_6	0.2406	-7.7531	-2.0609	-7.5435	-1.6425	-6.9149	-3.3163	-6.2862
RCLK2P	-7.4506	0.99	-6.1927	2.8748	-8.0795	0.7806	-4.7253	1.1995
EN8	-6.4347	-4.7747	-5.1776	-3.7275	-5.3871	-4.9841	-2.6633	-6.8691
HCLK1P	-5.4086	-6.7053	-1.0148	-7.334	-4.9901	-6.9149	-1.6425	-7.334
IO_I_1	-2.2443	-5.403	-6.4347	-6.2407	-3.0824	-1.4237	-6.2252	-4.7747
IO_I_2	-9.787	42.415	-3.0824	-1.6331	-2.6633	-3.0992	-5.3871	-3.7275
IO_I_3	-7.2728	-4.7747	-3.5014	-3.3086	-6.2252	-3.518	-2.6633	-1.0048
IO_I_4	-5.8061	-2.8897	-3.0824	-2.8897	-6.8537	-2.2614	-5.3871	-2.4708
IO_I_5	-2.2443	-4.9841	-0.9871	-2.052	-3.7109	-4.1464	-3.9204	-1.4237
LOADIN	-3.9204	-2.4708	-2.8728	-2.6803	-3.5014	-1.6331	-6.0156	0.0424
RCLK3P	-2.6633	-5.1936	-5.3871	-1.4237	-7.0632	-2.8897	-6.0156	-2.8897

Table 5b Single-ended I_{IL} (nA)

	2518		2519	
	Pre-Irra	Pos-Ann	Pre-Irra	Pos-Ann
DA	-8.3204	-8.3351	-7.4823	-8.1257
RCLK1P	-5.6804	-1.0202	-5.2615	-2.0674
IO_I_6	-1.6425	-5.448	-4.1532	-7.334
RCLK2P	-6.1927	2.2465	-6.1927	2.456
EN8	0.4795	-4.5652	-5.1776	-5.1936
HCLK1P	-1.4332	-7.1244	-2.4794	-6.7053
IO_I_1	-8.5299	-8.1257	-2.6633	-4.7747
IO_I_2	-4.549	-2.4708	-3.9204	-2.4708
IO_I_3	-3.7109	-3.3086	-3.7109	-3.518
IO_I_4	-7.2728	-0.3765	-0.3586	-1.0048
IO_I_5	-5.8061	-2.2614	-2.6633	-2.6803
LOADIN	-4.13	-2.052	-6.6442	-1.6331
RCLK3P	-8.5299	-1.8425	-4.549	-1.2142

Table 6a Single-ended I_{IH} (nA)

	2457		2460		2516		2517	
	Pre-Irra	Pos-Ann	Pre-Irra	Pos-Ann	Pre-Irra	Pos-Ann	Pre-Irra	Pos-Ann
DA	-1.1967	2.5557	5.0889	4.0218	-3.0824	2.9746	1.108	4.8595
RCLK1P	-0.4438	4.0066	2.0698	1.9121	-0.6532	2.1215	0.3941	4.6349
IO_I_6	2.1237	-3.1429	3.1698	-1.4665	0.659	-2.0952	1.7052	-3.1429
RCLK2P	2.8218	-3.8265	0.5158	-2.1512	3.0315	-3.4077	4.4989	-1.9418
EN8	-2.8728	-0.3765	2.9937	-0.5859	0.4795	1.7179	-4.3395	2.1368
HCLK1P	2.5421	-5.8671	5.4713	-5.2385	-1.4332	-4.6098	2.3329	-5.448
IO_I_1	-3.0824	-0.3765	5.508	-1.8425	2.9937	-0.5859	0.0604	1.9274
IO_I_2	-4.968	-1.8425	-2.4538	-1.6331	1.3176	-0.3765	-0.3586	-1.2142
IO_I_3	-6.2252	-0.5859	-2.2443	2.3462	0.4795	-2.4708	-3.5014	-0.7953
IO_I_4	-6.2252	0.4613	-4.968	0.0424	-3.0824	-0.7953	1.5271	0.4613
IO_I_5	-1.6157	-2.8897	-0.7776	1.299	-1.8252	-2.6803	-3.5014	-2.6803
LOADIN	-0.9872	-1.0048	-3.7109	-0.5859	-4.13	1.299	-2.2443	-1.8425
RCLK3P	1.7366	-1.4237	-0.9872	-2.4708	-0.7776	-1.8425	0.6890	-2.052

Table 6b Single-ended I_{IH} (nA)

	2518		2519	
	Pre-Irra	Pos-Ann	Pre-Irra	Pos-Ann
DA	3.2032	2.5557	1.9461	3.184
RCLK1P	4.1645	4.0066	2.0698	1.4932
IO_I_6	0.2406	-2.7238	-0.5963	0.2099
RCLK2P	2.8218	-3.8265	2.8218	-1.9418
EN8	0.27	0.2518	-3.5014	0.2518
HCLK1P	-2.6886	-2.7238	-1.4332	-5.2385
IO_I_1	-2.8728	1.5085	-1.6157	-1.0048
IO_I_2	0.27	2.1368	-2.6633	0.8802
IO_I_3	2.3652	0.0424	-1.4062	1.299
IO_I_4	3.4128	-0.167	0.2699	2.3462
IO_I_5	1.108	-1.6331	2.9937	-1.6331
LOADIN	-4.7585	-0.5859	1.108	-0.5859
RCLK3P	-3.0824	-2.052	-1.4062	-1.2142

D. Differential Input 3.3V-LVPECL V_{IL}/V_{IH} and I_{IL}

The LVPECL V_{IL}/V_{IH} is measured as the minimum differential voltage applied between P (positive) and N (negative) to generate a stable output Low/High respectively. For V_{IL} the differential is $V_N - V_P$, and for V_{IH} the differential is $V_P - V_N$. The applied common voltage ($\frac{V_P + V_N}{2}$) is 1.8V. The power supplies for V_{IL}/V_{IH} measurement are set as:

$$V_{CCA}/V_{CCI}/V_{PP}/V_{SV}/V_{KS} = 1.4/3.0/1.5/1.5/0.0 \text{ V}$$

The power supplies for I_{IL} measurement are set as:

$$V_{CCA}/V_{CCI}/V_{PP}/V_{SV}/V_{KS} = 1.5/3.3/1.5/1.5/0.0 \text{ V}$$

Tables 7a and 7b show the pre-irradiation and post-annealing tested data for V_{IL} of seven LVPECL inputs, and tables 8a and 8b show their pre-irradiation and post-annealing tested data for I_{IL}. Tables 9a and 9b show the pre-irradiation and post-annealing tested data for V_{IH} of seven LVPECL inputs. In every case, pre-irradiation or post-annealing, the tested data pass the spec of 0.3V.

Table7a LVPECL V_{IL} (mV)

	2457		2460		2516		2517	
	Pre-Irra	Pos-Ann	Pre-Irra	Pos-Ann	Pre-Irra	Pos-Ann	Pre-Irra	Pos-Ann
DIO_IP_1	80	152	90	90	80	80	80	80
DIO_IP_2	75	70	85	80	100	105	85	85
DIO_IP_3	85	92	90	90	85	85	95	100
DIO_IP_4	60	73	85	85	75	80	75	80
DIO_IP_5	75	86	95	95	95	95	90	90
DIO_IP_6	75	78	75	75	65	65	80	75
DIO_IP_7	95	80	80	80	80	80	80	90

Table7b LVPECL V_{IL} (mV)

	2518		2519	
	Pre-Irra	Pos-Ann	Pre-Irra	Pos-Ann
DIO_IP_1	85	85	80	80
DIO_IP_2	65	65	70	70
DIO_IP_3	85	85	90	90
DIO_IP_4	70	70	65	70
DIO_IP_5	95	95	85	85
DIO_IP_6	70	70	65	65
DIO_IP_7	80	80	85	90

Table 8a LVPECL I_{IL} (nA)

	2457		2460		2516		2517	
	Pre-Irra	Pos-Ann	Pre-Irra	Pos-Ann	Pre-Irra	Pos-Ann	Pre-Irra	Pos-Ann
DIO_IN_2	-6.7278	-4.5808	-5.471	-4.9997	-9.6603	-5.8375	-5.2615	-6.4658
DIO_IN_1	-6.8732	-10.2677	-7.9193	-11.9441	-5.1993	-12.3632	-6.2455	-15.5065
DIO_IN_3	-5.471	-1.6485	-5.2615	-3.5335	-5.6804	-1.0202	-5.2615	-2.2769
DIO_IP_1	-5.1993	-9.8486	-2.6886	-9.4295	-6.8732	-9.2199	-1.6425	-9.639
DIO_IN_4	-0.6532	0.446	-8.194	-2.2769	1.0225	0.0271	-2.9574	-1.4391
DIO_IN_5	-2.329	-2.6957	-5.6804	-0.6013	-4.6331	-1.0202	-4.8426	-2.2769
DIO_IN_6	-4.0047	-1.858	-4.6331	-2.0674	-6.5183	-0.1824	-4.8426	-2.2769
DIO_IN_7	-5.8899	-2.0674	-2.7479	-2.2769	-2.9574	-2.2769	-4.2142	-1.2296
DIO_IP_2	-4.0047	-2.6957	-1.0722	-0.8107	-3.3763	1.9121	-3.7952	-1.2296
DIO_IP_3	-1.4911	-1.6485	-6.0994	-2.0674	-6.5183	-3.3241	-2.1195	-0.6013
DIO_IP_4	-5.471	-3.3241	-4.4236	-2.9052	-3.7952	-3.9524	-2.1195	-2.6957
DIO_IP_5	-5.8899	-3.9524	-6.9372	-1.0202	-5.052	-3.1146	-1.2816	-3.1146
DIO_IP_6	-4.0047	-1.4391	-7.3562	-2.6957	-6.3088	-3.743	-3.3763	-4.1619
DIO_IP_7	-10.498	-1.858	-16.9916	-2.6957	-9.6603	-1.6485	-4.2142	-2.2769

Table 8b LVPECL I_{IL} (nA)

	2518		2519	
	Pre-Irra	Pos-Ann	Pre-Irra	Pos-Ann
DIO_IN_2	-2.9574	-4.1619	-6.7278	-4.1619
DIO_IN_1	-4.9901	-11.9441	-4.1532	-13.411
DIO_IN_3	-2.1195	-1.0202	-6.5183	-1.2296
DIO_IP_1	-5.1993	-10.4772	-4.3624	-10.2677
DIO_IN_4	-2.5384	-2.4863	-2.329	-0.8107
DIO_IN_5	-0.4438	-1.0202	-5.471	-1.6485
DIO_IN_6	-2.7479	-2.9052	-6.0994	-1.0202
DIO_IN_7	-3.7952	-2.6957	-5.2615	-1.6485
DIO_IP_2	-3.5858	-0.6013	-3.3763	-2.4863
DIO_IP_3	-4.8426	-3.9524	-0.0248	-2.2769
DIO_IP_4	-5.471	-1.4391	-5.052	-1.4391
DIO_IP_5	-6.3088	-2.0674	-0.6532	-2.2769
DIO_IP_6	-1.7006	-3.1146	-3.3763	-0.6013
DIO_IP_7	-6.0994	-1.858	-2.7479	-2.0674

Table 9a LVPECL V_{IH} (mV)

	2457		2460		2516		2517	
	Pre-Irra	Pos-Ann	Pre-Irra	Pos-Ann	Pre-Irra	Pos-Ann	Pre-Irra	Pos-Ann
DIO_IP_1	80	80	90	85	75	75	75	75
DIO_IP_2	75	80	85	85	105	105	85	90
DIO_IP_3	85	85	90	90	80	85	90	95
DIO_IP_4	75	75	95	95	85	85	80	85
DIO_IP_5	70	75	95	95	95	95	85	90
DIO_IP_6	85	85	85	85	80	80	80	90
DIO_IP_7	95	95	80	80	80	80	80	90

Table 9b LVPECL V_{IH} (mV)

	2518		2519	
	Pre-Irra	Pos-Ann	Pre-Irra	Pos-Ann
DIO_IP_1	85	85	80	80
DIO_IP_2	65	65	70	75
DIO_IP_3	80	85	85	90
DIO_IP_4	80	80	75	80
DIO_IP_5	95	95	80	85
DIO_IP_6	80	85	75	80
DIO_IP_7	80	85	85	85

E. 3.3V-LVTTL Output-Drive Voltage (V_{OL}/V_{OH})

The output drive voltage V_{OL}/V_{OH} is measured at an output pin when it is at Low/High state and sinking/sourcing 1.5 mA current respectively. The power supplies for V_{OL}/V_{OH} measurement are set as:

$$V_{CCA}/V_{CCI}/V_{PP}/V_{SV}/V_{KS} = 1.4/3.0/1.5/1.5/0.0 \text{ V}$$

The spec for V_{OL}/V_{OH} is < 0.4V/ >2.4V respectively. Table 10a and 10b show the pre-irradiation and post-annealing tested data for V_{OL}; in every case the V_{OL} data passes the spec. Table 11a and 11b show the pre-irradiation and post-annealing tested data for V_{OH}; in every case the V_{OH} data passes the spec.

Table 10a Single-ended V_{OL} (mV)

	2457		**2460**		**2516**		**2517**	
	Pre-Irr	Pos-An	Pre-Irr	Pos-An	Pre-Irr	Pos-An	Pre-Irr	Pos-An
QA_2	20	20	20	20	20	20	20	20
QA_1	20	20	20	20	20	20	20	20
QA_0	20	20	20	20	20	20	20	20
YQ_0	20	20	20	20	20	20	20	20
YQ_1	20	20	20	25	20	20	20	25
YQ_2	20	20	20	20	20	20	20	20
YQ_3	20	20	20	20	20	20	20	20
YQ_4	20	20	20	20	20	20	20	20
YQ_5	20	20	20	20	20	20	20	20
YQ_6	20	20	20	20	20	20	20	20
YQ_7	20	20	20	20	20	20	20	20
IO_O_1	25	20	25	20	25	20	25	20
IO_O_2	25	25	20	25	20	20	20	25
IO_O_3	20	20	25	20	25	20	25	20
IO_O_4	20	20	20	20	20	20	20	20
IO_O_5	25	20	25	20	25	20	25	20
IO_O_6	20	20	20	20	25	25	25	25
O_ANDC_CLKF	25	25	25	25	30	25	35	25
O_ANDC_CLKG	25	25	25	25	30	25	30	25
O_ANDC_HCLKA	25	25	25	25	25	25	25	25
O_ANDP_CLKF	30	25	30	25	30	30	30	30
O_ANDP_CLKG	30	30	30	30	30	30	30	30
O_ANDP_HCLKA	35	30	30	30	40	30	35	30
O_ORC_CLKF	25	25	25	25	25	25	25	25
O_ORC_CLKG	25	25	25	25	25	25	25	25
O_ORC_HCLKA	25	25	25	25	25	25	25	25
O_ORP_CLKF	30	30	25	30	40	25	30	25
O_ORP_CLKG	30	30	30	25	35	30	30	25
O_ORP_HCLKA	30	30	30	30	30	30	30	30
O_FF_CLKF	35	30	30	30	45	30	40	30
O_FF_CLKG	40	30	30	30	75	35	65	30
O_FF_HCLKA	40	30	30	25	85	40	60	30

Table 10b Single-ended V_{OL} (mV)

	2518		2519	
	Pre-Irr	Pos-An	Pre-Irr	Pos-An
QA_2	20	20	20	20
QA_1	20	20	20	20
QA_0	20	20	20	20
YQ_0	20	20	20	20
YQ_1	20	20	20	25
YQ_2	20	20	20	20
YQ_3	20	20	20	20
YQ_4	20	20	20	20
YQ_5	20	20	20	20
YQ_6	20	20	20	20
YQ_7	20	20	20	20
IO_O_1	25	20	25	20
IO_O_2	25	20	25	20
IO_O_3	25	20	25	20
IO_O_4	20	20	20	25
IO_O_5	25	20	25	20
IO_O_6	20	20	25	25
O_ANDC_CLKF	25	70	55	35
O_ANDC_CLKG	25	55	40	30
O_ANDC_HCLKA	25	25	25	25
O_ANDP_CLKF	30	30	30	30
O_ANDP_CLKG	30	25	30	25
O_ANDP_HCLKA	30	35	45	30
O_ORC_CLKF	25	25	25	25
O_ORC_CLKG	25	25	25	25
O_ORC_HCLKA	25	25	25	25
O_ORP_CLKF	25	40	35	30
O_ORP_CLKG	30	35	30	25
O_ORP_HCLKA	30	30	30	30
O_FF_CLKF	30	70	35	30
O_FF_CLKG	30	215	65	40
O_FF_HCLKA	30	170	60	35

Table 11a Single-ended V_{OH} (V)

	2457		2460		2516		2517	
	Pre-Irr	Pos-An	Pre-Irr	Pos-An	Pre-Irr	Pos-An	Pre-Irr	Pos-An
QA_2	2.97	2.965	2.97	2.965	2.97	2.965	2.97	2.97
QA_1	2.97	2.965	2.97	2.965	2.97	2.965	2.97	2.97
QA_0	2.97	2.965	2.97	2.965	2.965	2.965	2.97	2.97
YQ_0	2.98	2.96	3.01	2.96	3.01	2.96	3	2.965
YQ_1	2.98	2.96	3.01	2.96	3.01	2.96	3	2.965
YQ_2	2.97	2.96	3.01	2.96	3.01	2.96	3	2.965
YQ_3	2.97	2.965	3.015	2.965	3.01	2.965	3	2.965
YQ_4	2.97	2.96	3.01	2.96	3.01	2.96	2.995	2.965
YQ_5	2.99	2.96	3.01	2.96	3.01	2.96	3	2.96
YQ_6	2.99	2.965	3.015	2.96	3.01	2.96	3	2.965
YQ_7	2.97	2.96	3.01	2.96	3.01	2.96	3	2.965
IO_O_1	2.98	2.965	3.01	2.965	3.01	2.965	3	2.965
IO_O_2	2.97	2.965	3.01	2.965	3.01	2.965	3	2.97
IO_O_3	2.985	2.965	3.01	2.965	3.01	2.965	3	2.965
IO_O_4	2.98	2.965	3.01	2.965	3.005	2.965	3	2.97
IO_O_5	2.975	2.965	3.01	2.965	3.01	2.965	3	2.97
IO_O_6	2.975	2.965	3.015	2.965	3.01	2.965	3	2.97
O_ANDC_CLKF	2.965	2.965	2.97	2.965	2.965	2.965	2.945	2.965
O_ANDC_CLKG	2.965	2.97	2.97	2.97	2.96	2.97	2.95	2.97
O_ANDC_HCLKA	2.97	2.965	2.965	2.965	2.965	2.965	2.97	2.97
O_ANDP_CLKF	2.975	2.97	2.975	2.97	2.975	2.97	2.975	2.975
O_ANDP_CLKG	2.97	2.975	2.97	2.975	2.97	2.975	2.97	2.975
O_ANDP_HCLKA	2.97	2.97	2.97	2.97	2.94	2.97	2.965	2.975
O_ORC_CLKF	2.97	2.97	2.97	2.97	2.97	2.97	2.97	2.97
O_ORC_CLKG	2.975	2.965	2.97	2.965	2.97	2.965	2.97	2.97
O_ORC_HCLKA	2.97	2.965	2.965	2.965	2.965	2.965	2.97	2.965
O_ORP_CLKF	2.97	2.975	2.97	2.975	2.945	2.97	2.96	2.97
O_ORP_CLKG	2.97	2.97	2.97	2.97	2.94	2.97	2.96	2.97
O_ORP_HCLKA	2.975	2.975	2.965	2.97	2.965	2.97	2.97	2.975
O_FF_CLKF	2.975	2.97	2.97	2.97	2.93	2.97	2.97	2.97
O_FF_CLKG	2.97	2.975	2.97	2.975	2.92	2.975	2.945	2.97
O_FF_HCLKA	2.97	2.97	2.975	2.97	2.92	2.97	2.955	2.97

Table 11b Single-ended V_{OH} (V)

	2518		2519	
	Pre-Irr	Pos-An	Pre-Irr	Pos-An
QA_2	2.97	2.97	2.97	2.97
QA_1	2.97	2.97	2.97	2.97
QA_0	2.97	2.965	2.97	2.97
YQ_0	2.985	2.965	3	2.965
YQ_1	2.985	2.965	3	2.965
YQ_2	2.98	2.965	3	2.965
YQ_3	2.985	2.965	3.005	2.965
YQ_4	2.98	2.965	2.995	2.965
YQ_5	2.985	2.96	3	2.96
YQ_6	2.985	2.965	3	2.965
YQ_7	2.98	2.965	3	2.965
IO_O_1	2.985	2.965	3	2.965
IO_O_2	2.985	2.965	3	2.97
IO_O_3	2.985	2.965	3	2.965
IO_O_4	2.985	2.97	3	2.97
IO_O_5	2.985	2.97	3	2.97
IO_O_6	2.985	2.965	3.005	2.965
O_ANDC_CLKF	2.97	2.91	2.945	2.965
O_ANDC_CLKG	2.97	2.9	2.94	2.965
O_ANDC_HCLKA	2.97	2.97	2.97	2.97
O_ANDP_CLKF	2.975	2.97	2.97	2.97
O_ANDP_CLKG	2.975	2.975	2.975	2.975
O_ANDP_HCLKA	2.97	2.94	2.945	2.965
O_ORC_CLKF	2.97	2.97	2.97	2.97
O_ORC_CLKG	2.975	2.97	2.97	2.97
O_ORC_HCLKA	2.97	2.965	2.97	2.965
O_ORP_CLKF	2.97	2.93	2.95	2.965
O_ORP_CLKG	2.97	2.92	2.95	2.96
O_ORP_HCLKA	2.97	2.975	2.97	2.975
O_FF_CLKF	2.975	2.94	2.935	2.965
O_FF_CLKG	2.975	2.97	2.87	2.945
O_FF_HCLKA	2.975	2.97	2.895	2.955

F. 3.3V-LVPECL Output-Drive Voltage (V_{OL}/V_{OH})

The output drive voltage V_{OL}/V_{OH} is measured at an output pin when it is at Low/High state and sinking/sourcing 1.5 mA current respectively. The spec for 3.3 V-LVPEL V_{OL}/V_{OH} is < 0.4V/ >2.4V respectively. The power supplies for V_{OL}/V_{OH} measurement are set as:

$$V_{CCA}/V_{CCI}/V_{PP}/V_{SV}/V_{KS} = 1.4/3.0/1.5/1.5/0.0 \text{ V}$$

Table 12a and 12b show the pre-irradiation and post-annealing tested data for 3.3 V-LVPEL V_{OL}; in every case the V_{OL} data passes the spec. Table 13a and 13b show the pre-irradiation and post-annealing tested data for 3.3 V-LVPEL V_{OH}; in every case the V_{OH} data passes the spec.

Table 12a LVPECL V_{OL} (mV)

	2457		2460		2516		2517	
	Pre-Irra	Pos-Ann	Pre-Irra	Pos-Ann	Pre-Irra	Pos-Ann	Pre-Irra	Pos-Ann
DIO_O_1	20	20	20	20	20	20	20	20
DIO_O_2	20	20	20	20	20	20	20	20
DIO_O_3	20	20	20	20	20	20	20	20
DIO_O_4	20	20	20	20	20	20	20	20
DIO_O_5	20	20	20	20	20	20	20	20
DIO_O_6	20	20	20	20	20	20	20	20
DIO_O_7	20	20	20	20	20	20	20	20

Table 12b LVPECL V_{OL} (mV)

	2518		2519	
	Pre-Irra	Pos-Ann	Pre-Irra	Pos-Ann
DIO_O_1	20	20	20	20
DIO_O_2	20	20	20	20
DIO_O_3	20	20	20	20
DIO_O_4	20	20	20	20
DIO_O_5	20	20	20	20
DIO_O_6	20	20	20	20
DIO_O_7	20	20	20	20

Table 13a LVPECL V_{OH} (V)

	2457		2460		2516		2517	
	Pre-Irra	Pos-Ann	Pre-Irra	Pos-Ann	Pre-Irra	Pos-Ann	Pre-Irra	Pos-Ann
DIO_O_1	2.975	2.97	3	2.97	3	2.97	2.99	2.97
DIO_O_2	2.97	2.97	3	2.97	2.995	2.965	2.99	2.97
DIO_O_3	2.97	2.97	3	2.965	3	2.965	2.99	2.97
DIO_O_4	2.975	2.97	3	2.97	3	2.97	2.99	2.965
DIO_O_5	2.99	2.97	3	2.97	3	2.965	2.99	2.97
DIO_O_6	2.995	2.965	2.995	2.965	3	2.965	2.99	2.965
DIO_O_7	2.975	2.97	3	2.965	3	2.965	2.99	2.965

Table 13b LVPECL V_{OH} (V)

	2518		2519	
	Pre-Irra	Pos-Ann	Pre-Irra	Pos-Ann
DIO_O_1	2.98	2.97	2.99	2.97
DIO_O_2	2.98	2.97	2.99	2.97
DIO_O_3	2.98	2.965	2.99	2.965
DIO_O_4	2.98	2.97	2.99	2.97
DIO_O_5	2.98	2.97	2.99	2.97
DIO_O_6	2.98	2.965	2.99	2.965
DIO_O_7	2.98	2.965	2.99	2.965

G. *Propagation Delay*

The propagation delay was measured post-irradiation, and post-annealing. The irradiation was temporarily stopped at each total-dose increment of 100 krad for the measurement. Each measurement has a 1-minutes wait following the irradiation shut-down. The results are plotted in Figure 9, and also listed in Table 14. As shown in Figure 9, the propagation delay initially decreases with the total dose and then increases. However, as listed in Table 14, the change is small throughout the irradiation. Referring to in-flux static current plots (Figure 3 to 8), the device might heat up as the dose increases. The rising temperature could be the root cause of the increasing trend at high total dose.

The post-annealing data, on the other hand, always show decreased delay in every case.

The radiation delta in every case is well within the 10% degradation criterion. User can take the worst case for design-margin consideration.

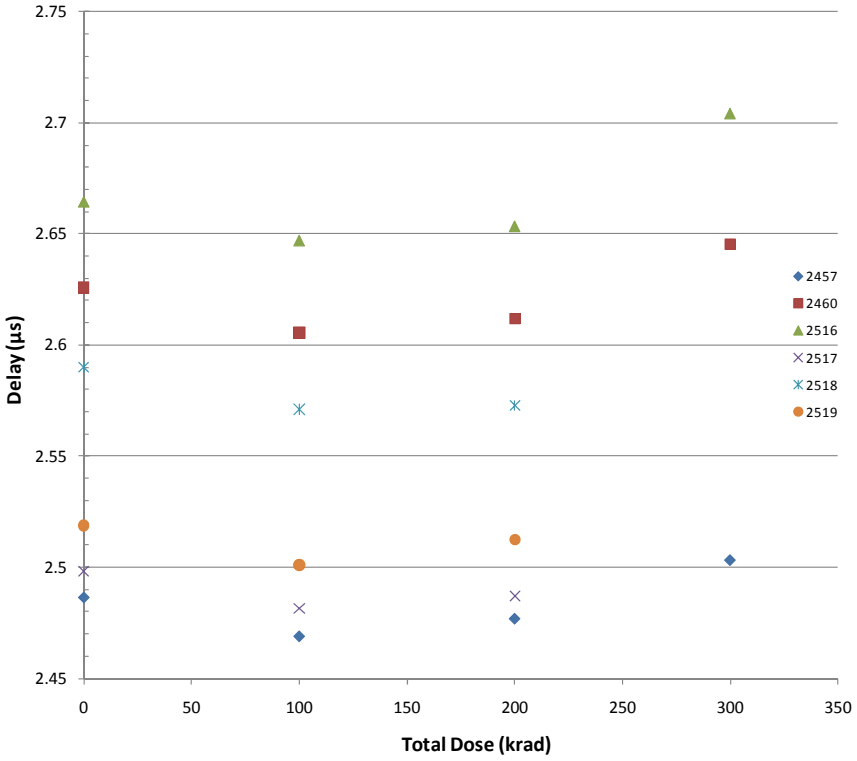

Figure 9 In-situ propagation delay versus total dose. The measurement was performed when irradiation was temporarily stopped.

Table 14 Radiation-Induced Propagation Delay Degradations

DUT		Pre-rad	100 krad	200 krad	300 krad	Post-ann
2457	Delay (µs)	2.4865	2.4691	2.477	2.5032	2.4591
	Radiation Δ	NA	-0.70%	-0.38%	0.67%	-1.10%
2460	Delay (µs)	2.6258	2.6056	2.6119	2.6453	2.5906
	Radiation Δ	NA	-0.77%	-0.53%	0.74%	-1.34%
2516	Delay (µs)	2.6643	2.6468	2.6532	2.7041	2.6361
	Radiation Δ	NA	-0.66%	-0.42%	1.49%	-1.06%
2517	Delay (µs)	2.4983	2.4816	2.4871	NA	2.4689
	Radiation Δ	NA	-0.67%	-0.45%	NA	-1.18%
2518	Delay (µs)	2.5901	2.571	2.5728	NA	2.5548
	Radiation Δ	NA	-0.74%	-0.67%	NA	-1.36%
2519	Delay (µs)	2.5187	2.501	2.5123	NA	2.4945
	Radiation Δ	NA	-0.70%	-0.25%	NA	-0.96%

H. Transition Time

Figures 10 to 21 show the pre-irradiation and post-annealing transition edges. In each case, the radiation-induced transition-time degradation is insignificant.

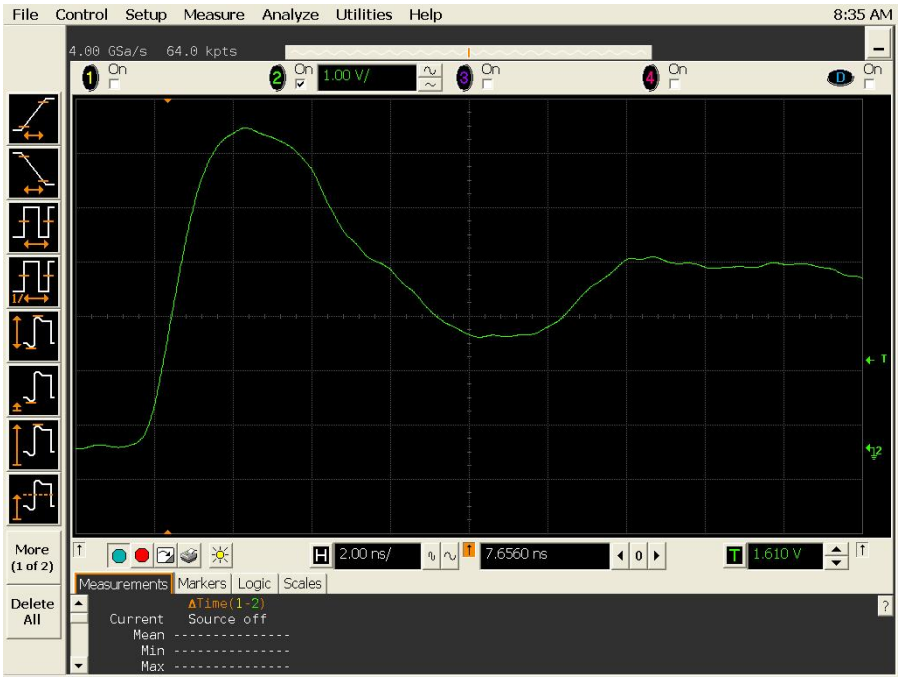

Figure 10(a) DUT 2457 pre-irradiation rising edge.

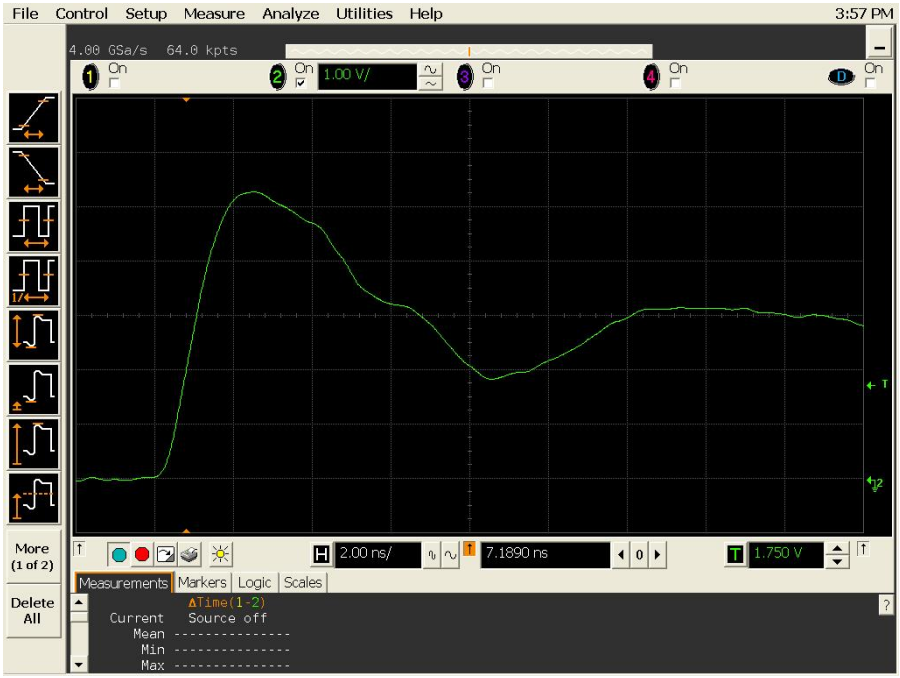

Figure 10(b) DUT 2457 post-annealing rising edge.

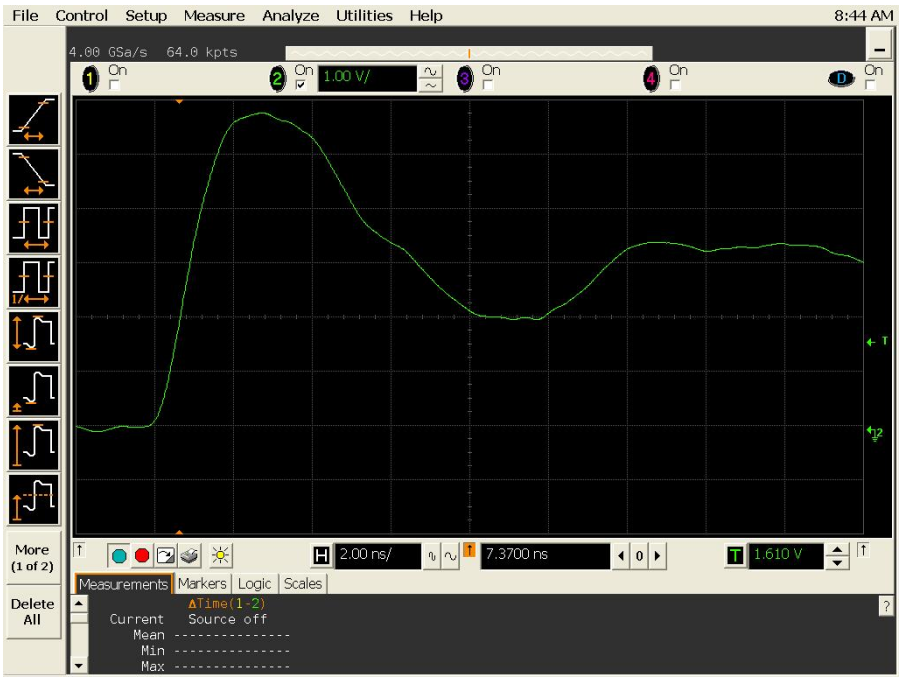

Figure 11(a) DUT 2460 pre-irradiation rising edge.

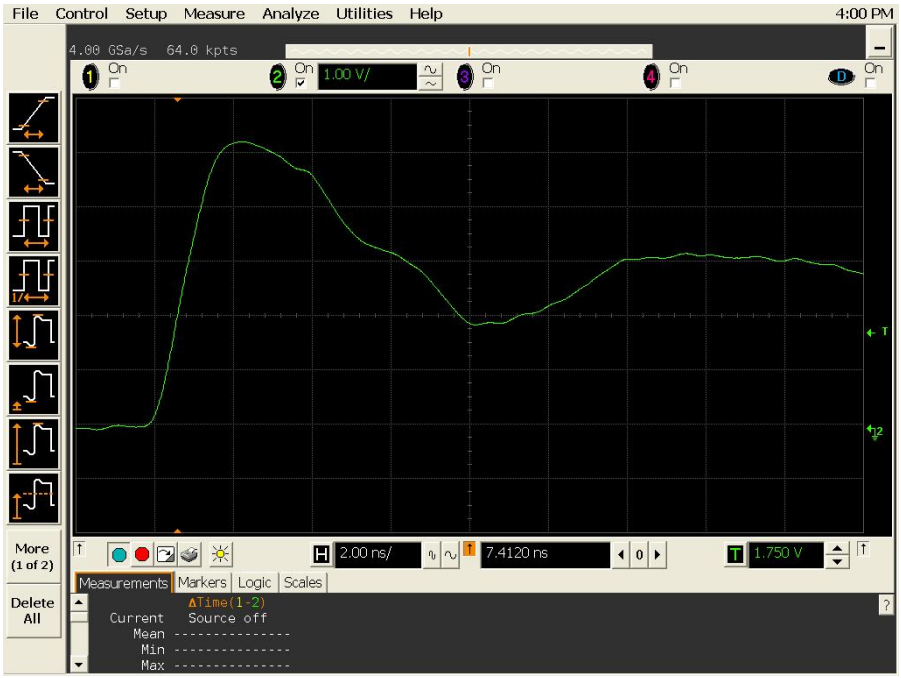

Figure 11(b) DUT 2460 post-annealing rising edge.

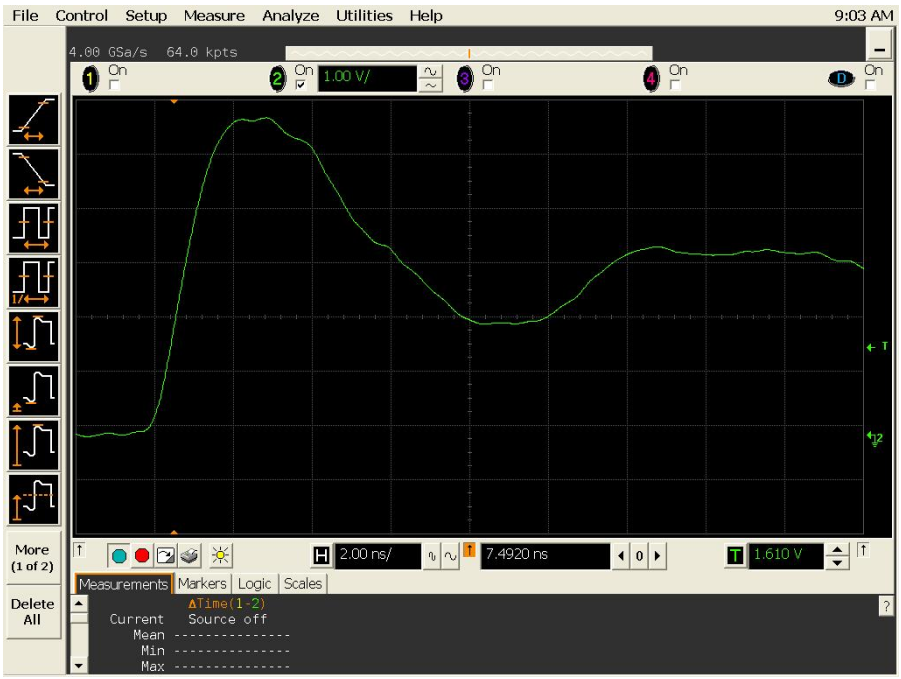

Figure 12(a) DUT 2516 pre-radiation rising edge.

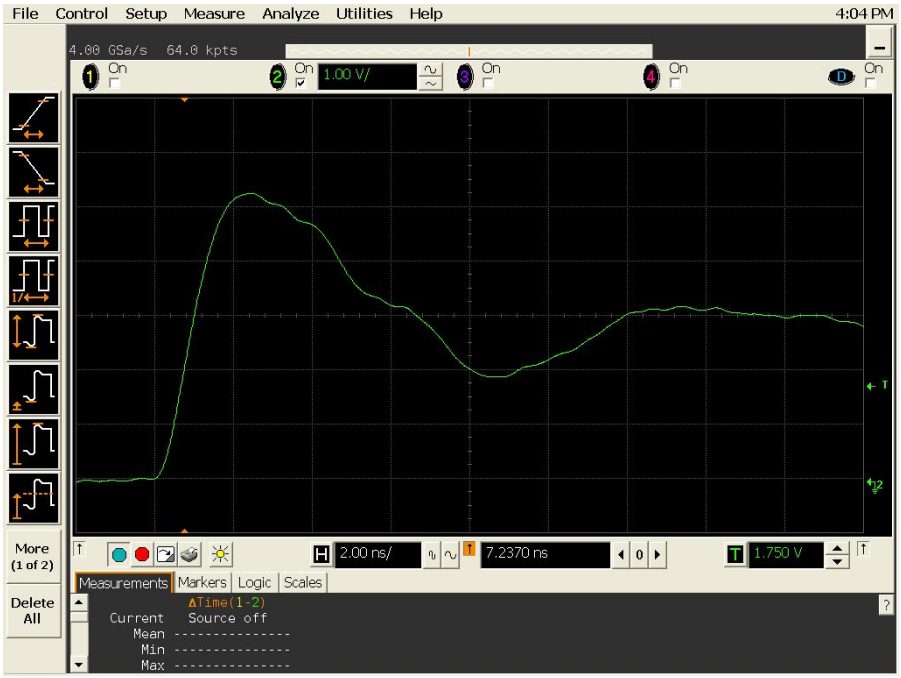

Figure 12(b) DUT 2516 post-annealing rising edge.

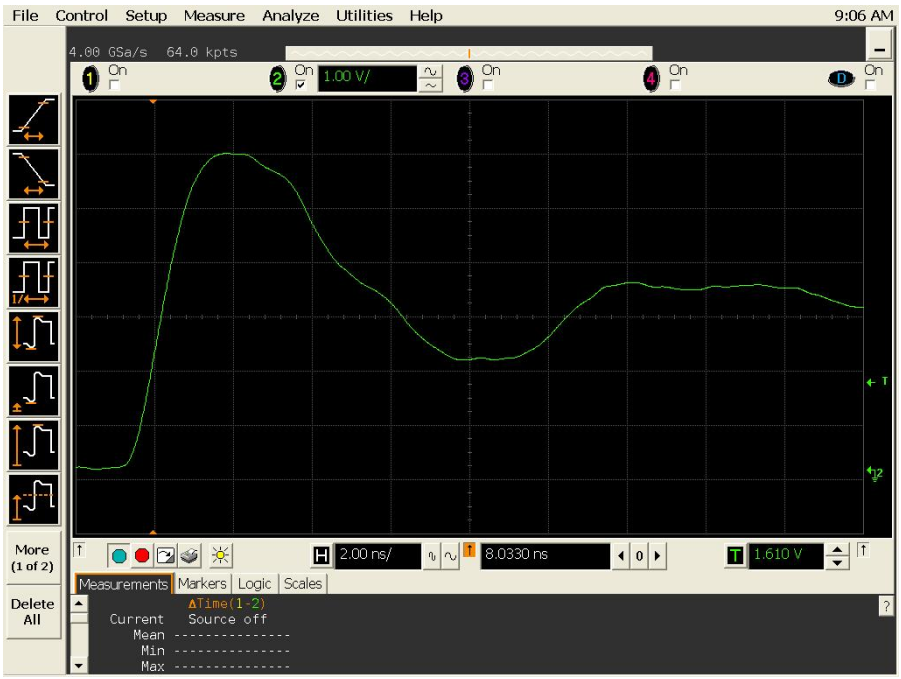

Figure 13(a) DUT 2517 pre-irradiation rising edge.

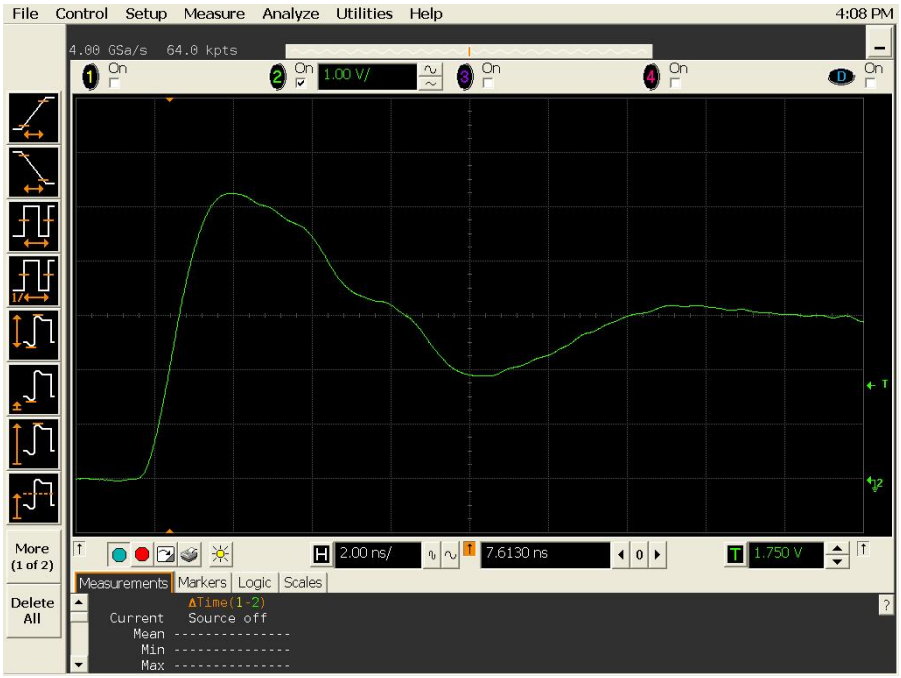

Figure 13(b) DUT 2517 post-annealing rising edge.

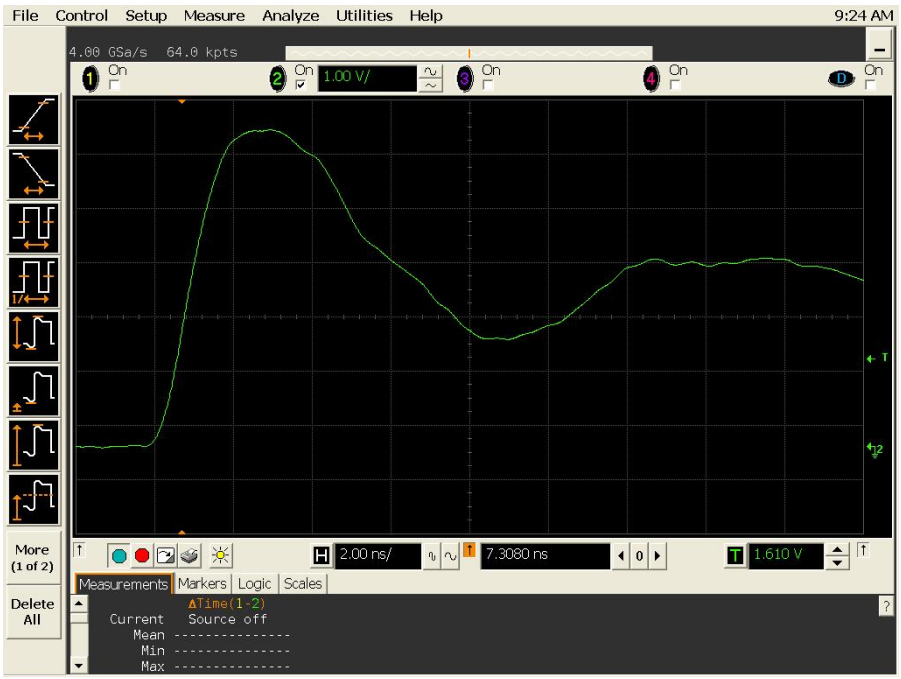

Figure 14(a) DUT 2518 pre-irradiation rising edge.

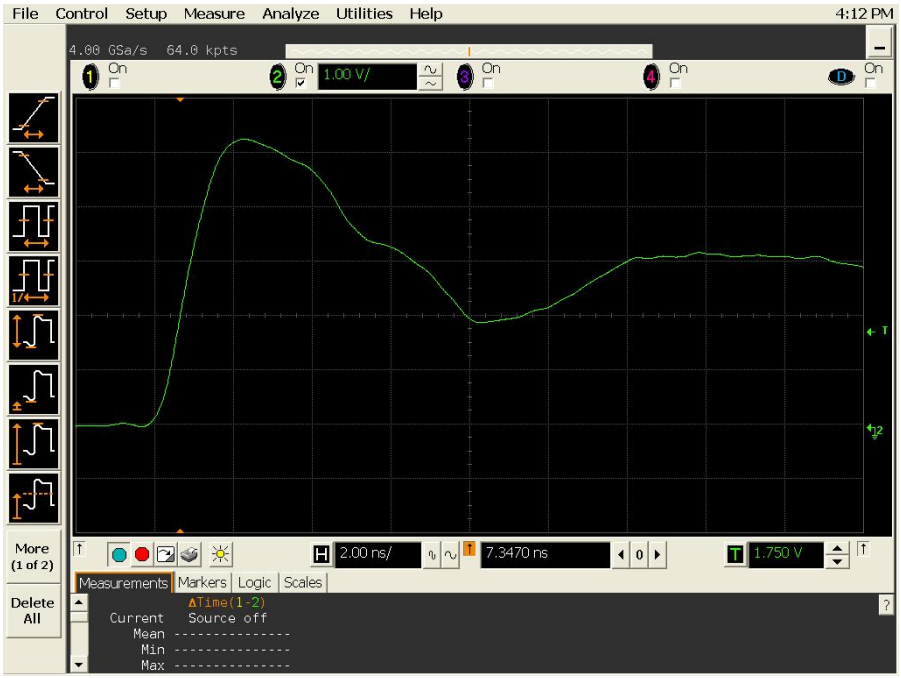

Figure 14(b) DUT 2518 post-annealing rising edge.

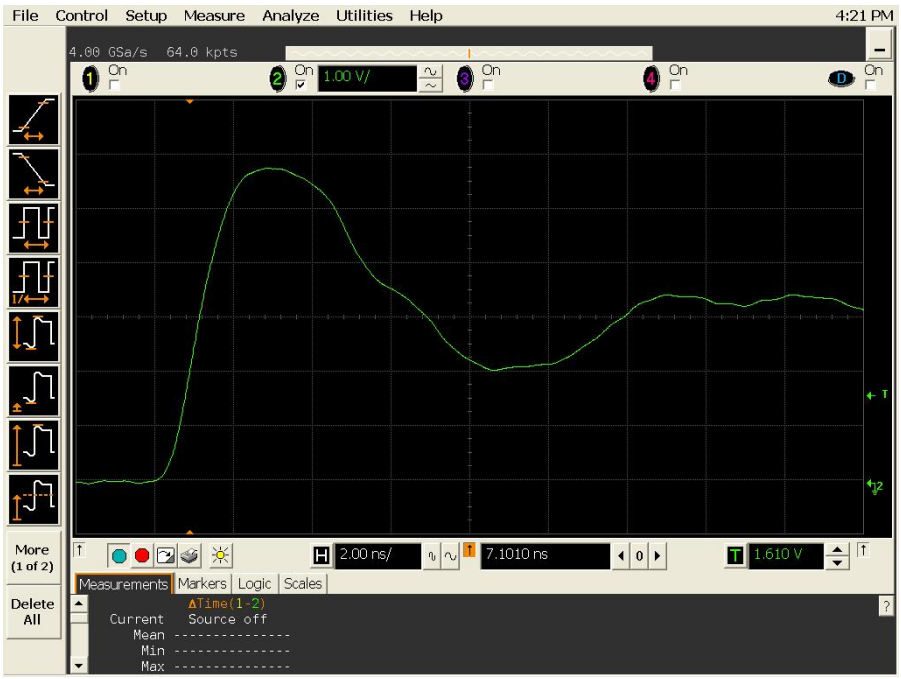

Figure 15(a) DUT 2519 pre-irradiation rising edge.

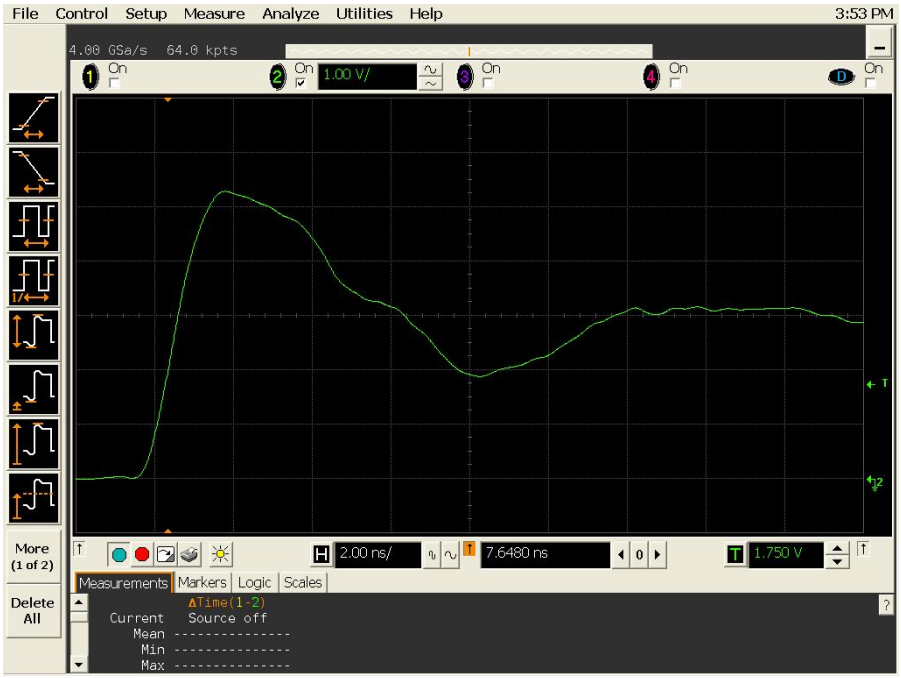

Figure 15(b) DUT 2519 post-annealing rising edge.

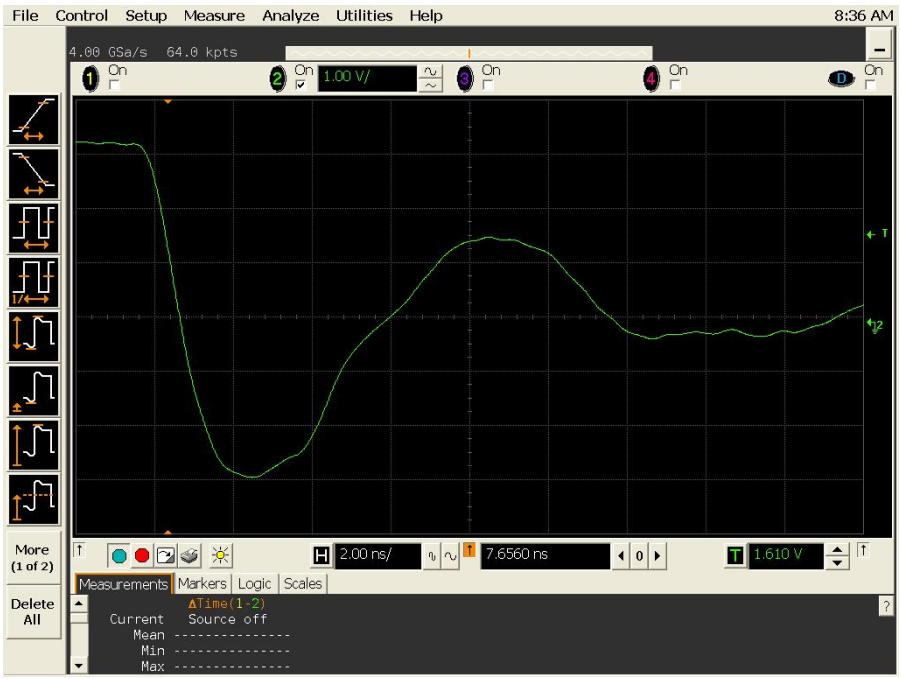

Figure 16(a) DUT 2457 pre-irradiation falling edge.

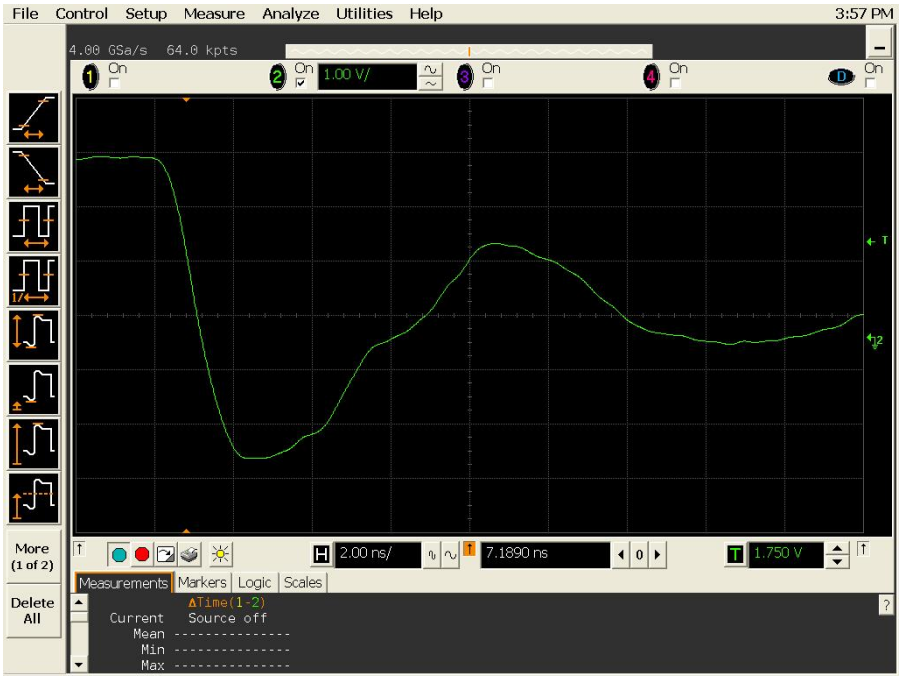

Figure 16(b) DUT 2457 post-annealing falling edge.

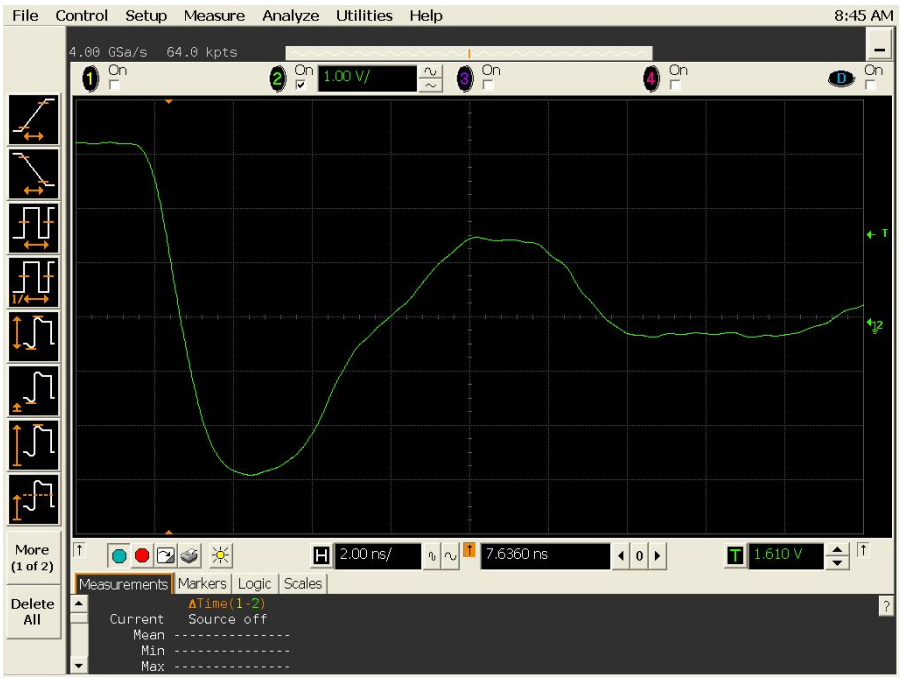

Figure 17(a) DUT 2460 pre-irradiation falling edge.

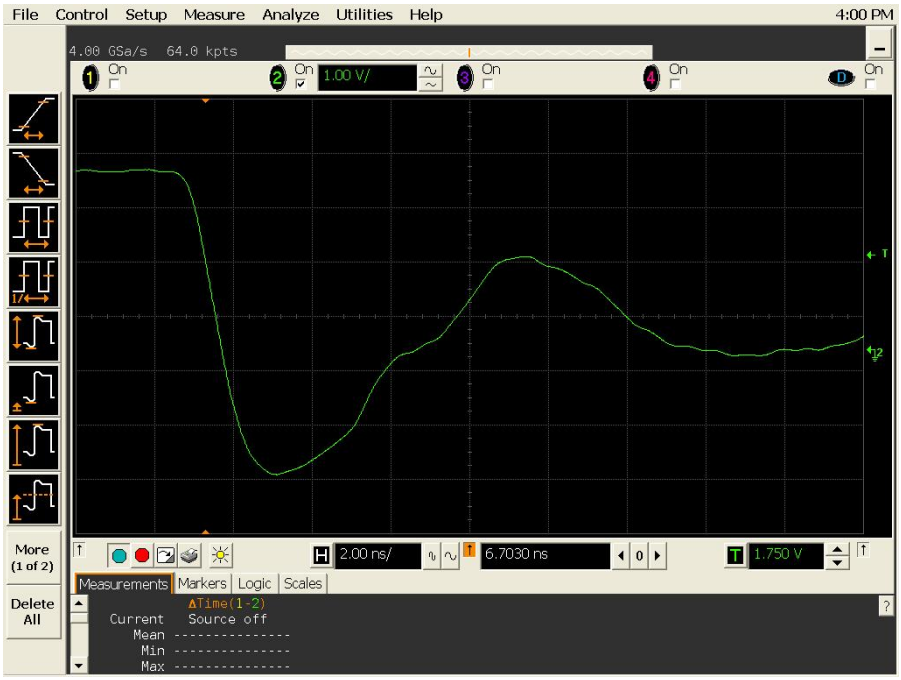

Figure 17(b) DUT 2460 post-annealing falling edge.

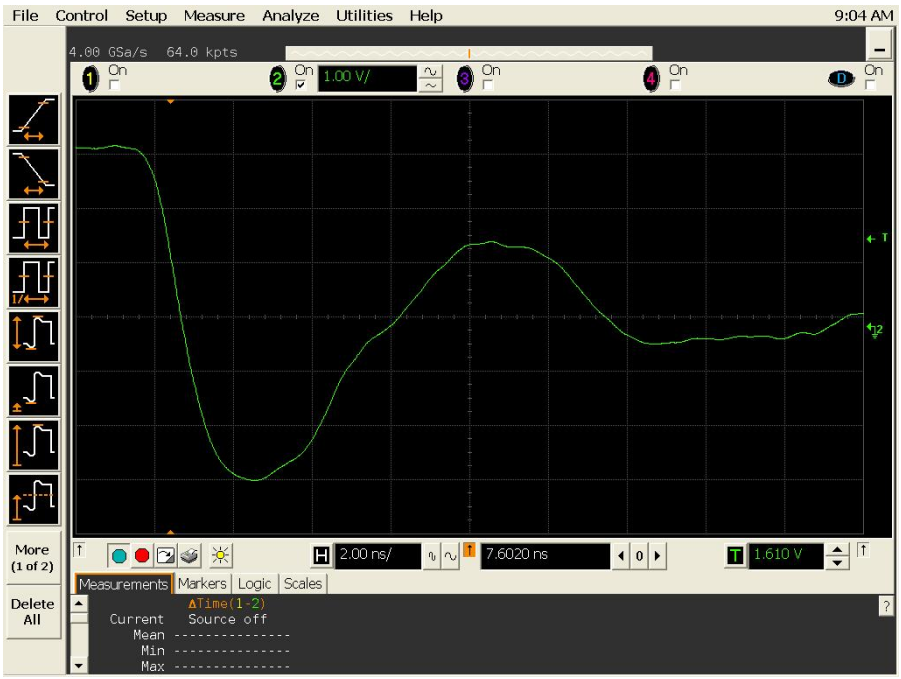

Figure 18(a) DUT 2516 pre-irradiation falling edge.

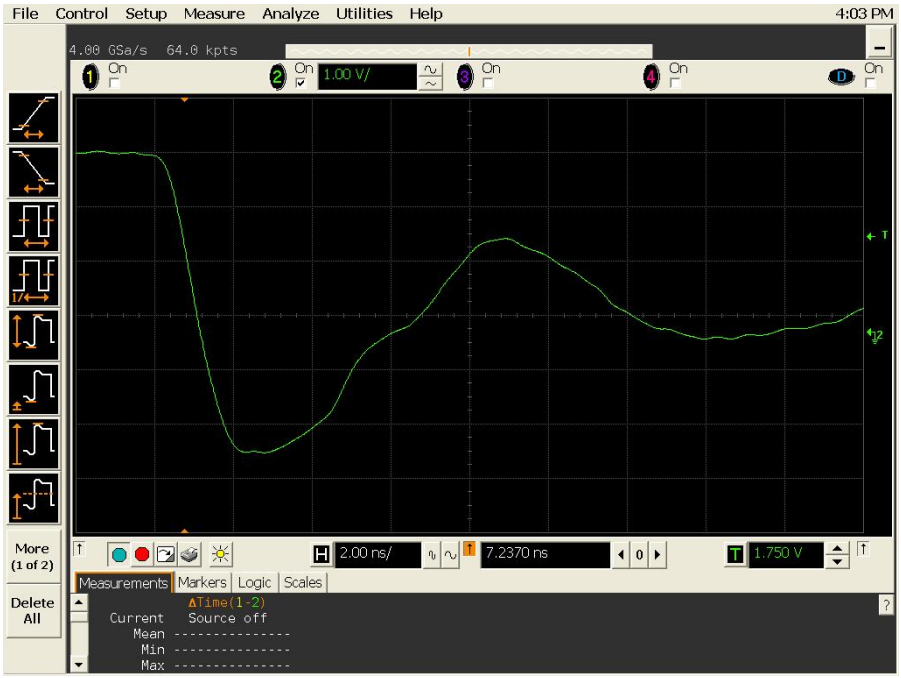

Figure 18(b) DUT 2516 post-annealing falling edge.

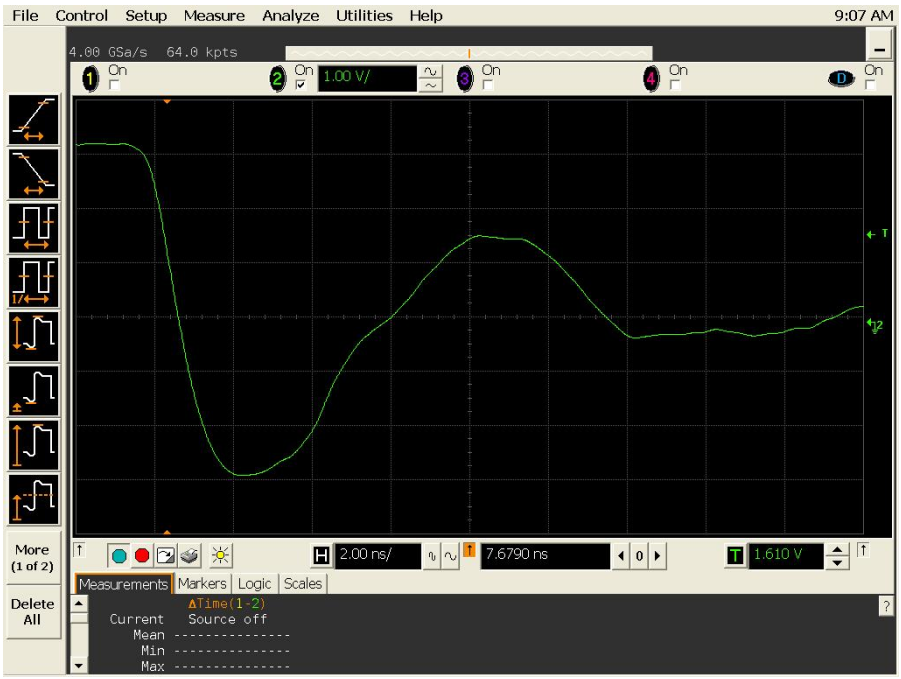

Figure 19(a) DUT 2517 pre-irradiation falling edge.

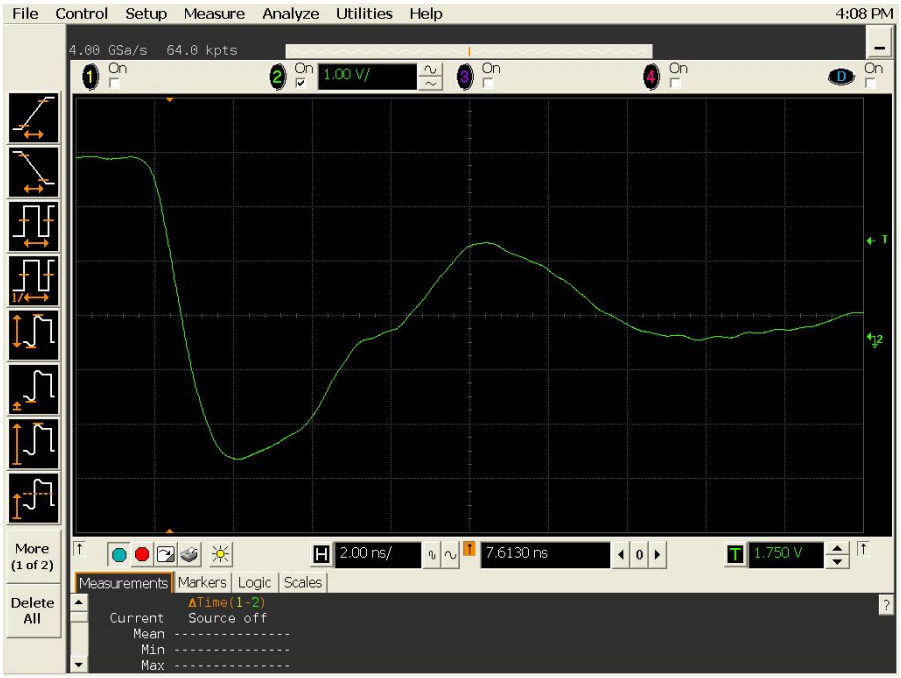

Figure 19(b) DUT 2517 post-annealing falling edge.

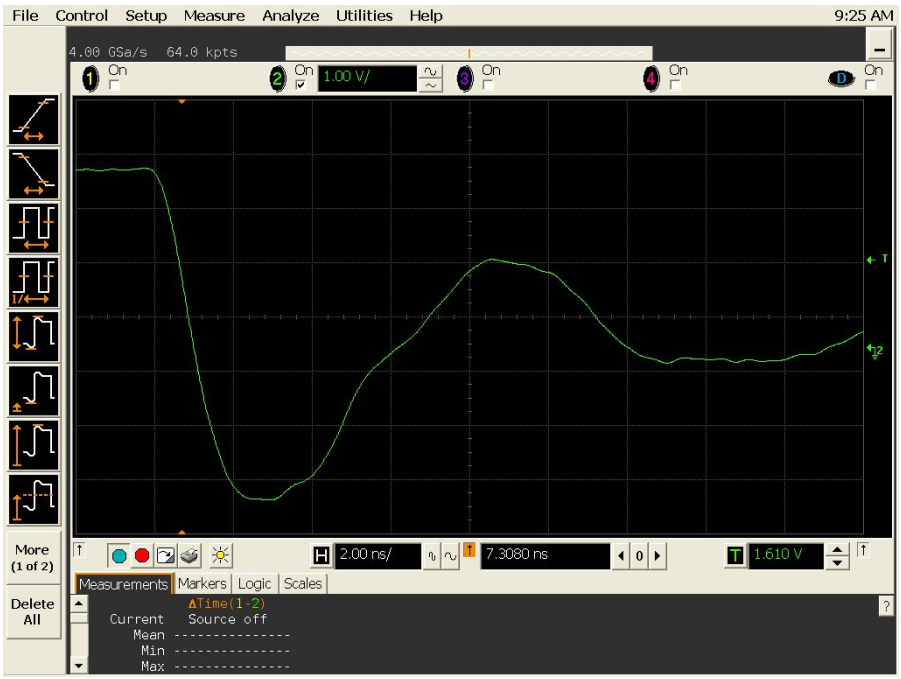

Figure 20(a) DUT 2518 pre-irradiation falling edge.

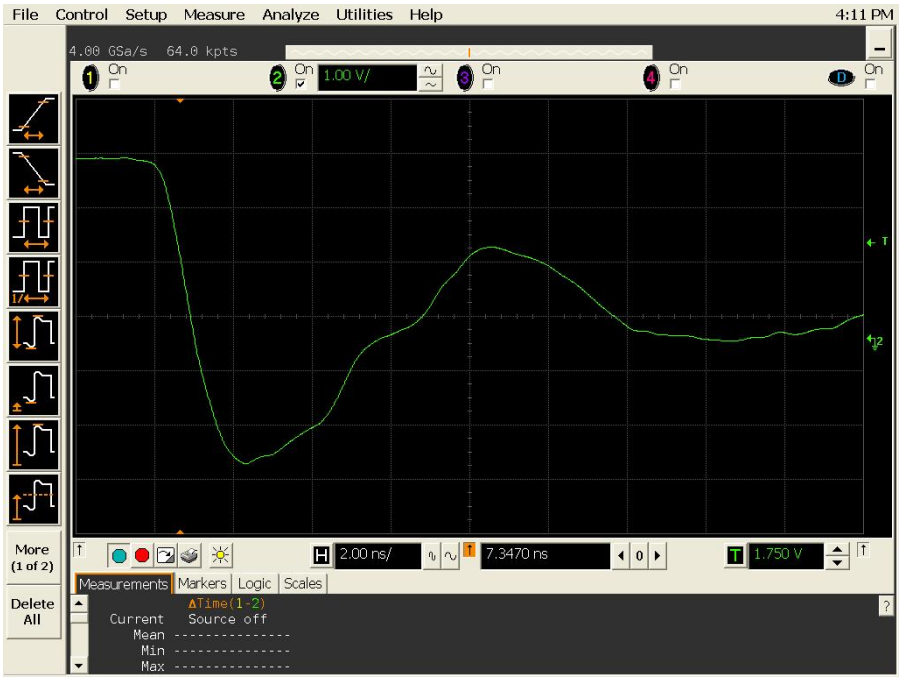

Figure 20(b) DUT 2518 post-annealing falling edge.

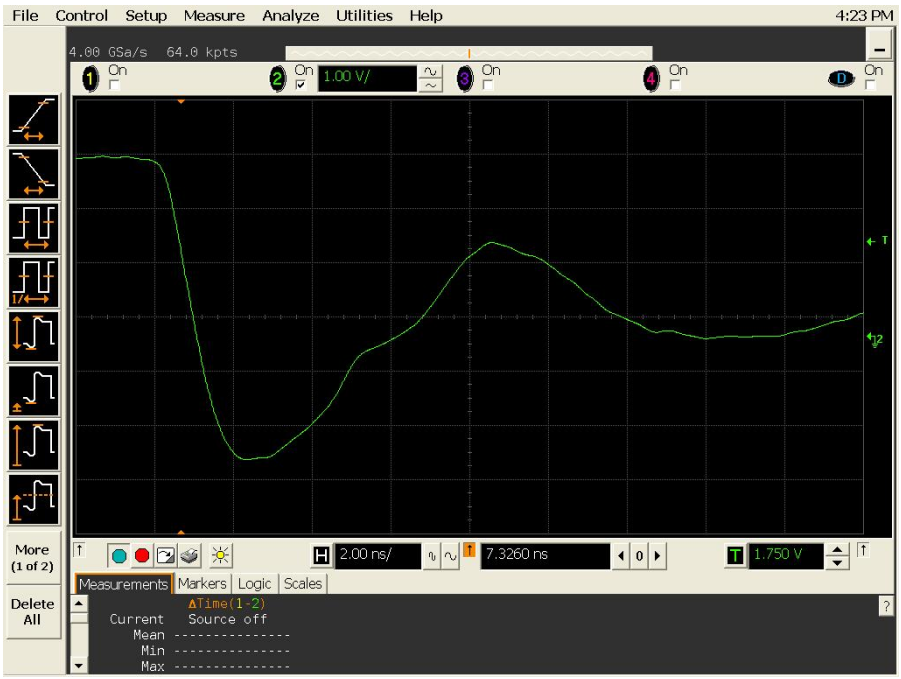

Figure 21(a) DUT 2519 pre-irradiation falling edge.

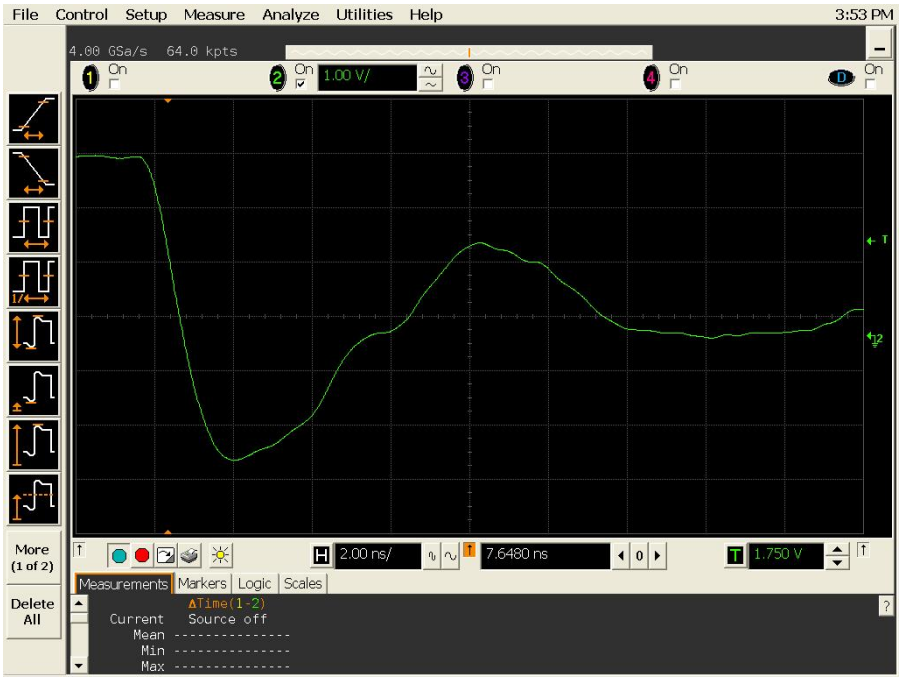

Figure 21(b) DUT 2519 post-annealing falling edge.